OCEAN 621
5/20-22/09

DEEP-SEA REDUCING HABITATS

1) Definition

2) Hydrothermal vents

   a. History of discovery

   b. Physical characteristics of Vents

   c. Hydrothermal vent microbiology

   d. Nature of vent communities

      - High local biomass

      - Exotic nature of fauna

      - Unusual feeding modes - endosymbiotic chemoautotrophy

      - Dynamism of communities

3) Other reducing habitats

   a. Shallow water

   b. Deep sea ("Cold Seeps")

      - Subduction zones

- Petroleum seeps
- Turbidites/canyons
- Base of carbonate scarp
- Anoxic basins
- Deep-Sea Whale falls

Reducing Habitat = a habitat where energy from reduced inorganic chemical species (e.g., H_2S, H_2, CH_4) is converted, via microbial endosymbiosis, into biomass of higher organisms.

NB. The occurrence of reducing habitats is generally dependent on the availability of reduced chemicals and oxygen in close proximity (scale of centimeters).

“Some energy source and sink are clearly needed if organisms are to function. … The internal heat of a planet, mostly of radioactive origin, in theory would provide an alternative to incoming radiation though we have little precedent as to how an organism could use it.”

G. Evelyn Hutchinson, *The Ecological Theater and the Evolutionary Play,* 1965, Yale Univ Press.

Reading:

Van Dover et al., 2002. Evolution and biogeography of deep-sea vent and seep invertebrates. *Science* 295: 1253-7

Smith, C. R. 2006. Bigger is better: The role of whales as detritus in marine ecosystems. In*: Whales, Whaling and Ocean Ecosystems,* J.A. Estes et al., eds. University of California Press, pp. 286 – 301.

General reference:

Van Dover, C. L. 2000. *The Ecology of Deep-Sea Hydrothermal Vents.* Princeton Univ. Press.

Typical Deep-Sea Floor

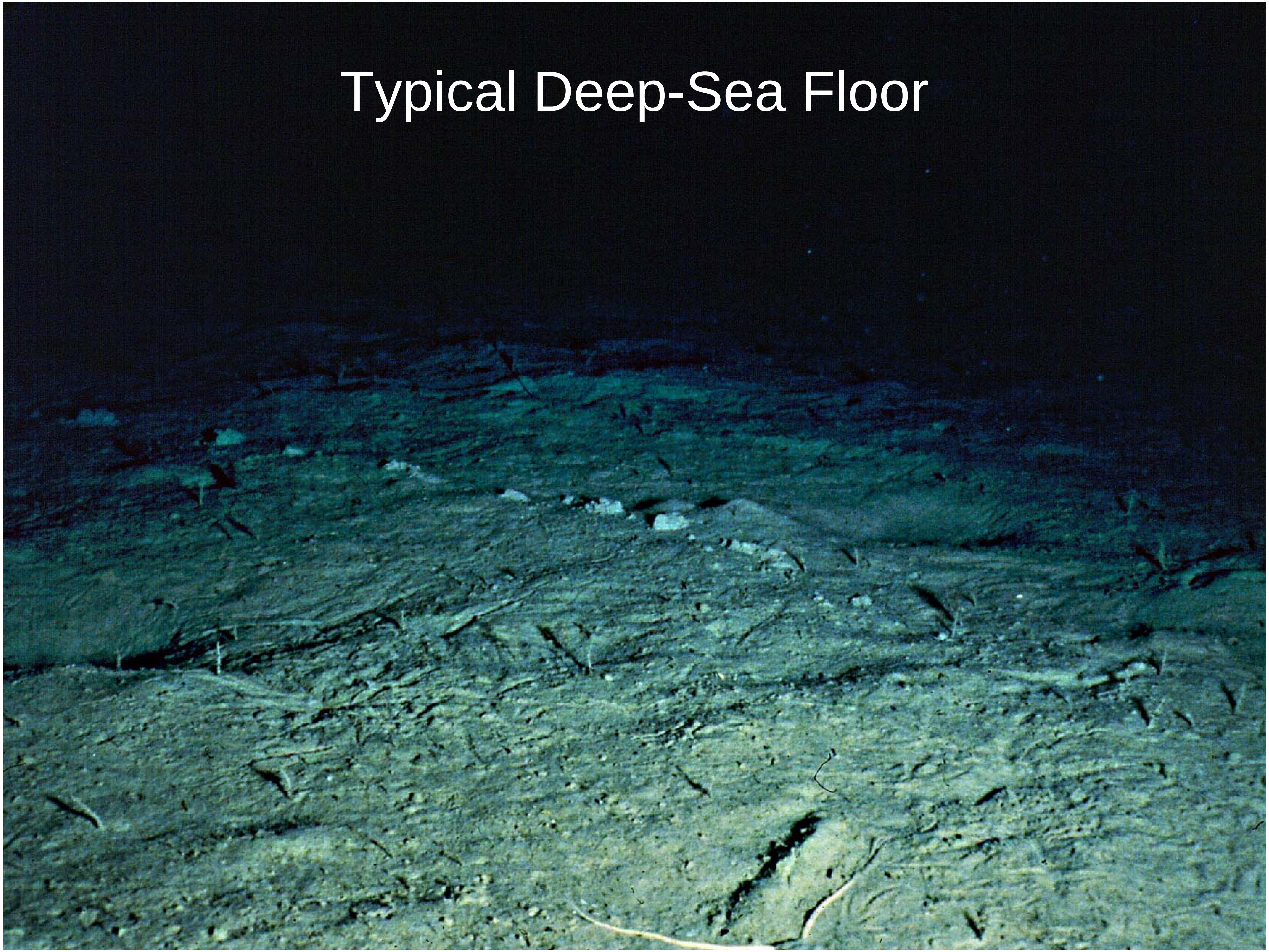

Most Nonvent Macrofaunal Species are Tiny Deposit Feeders

(esp. surface deposit feeders)

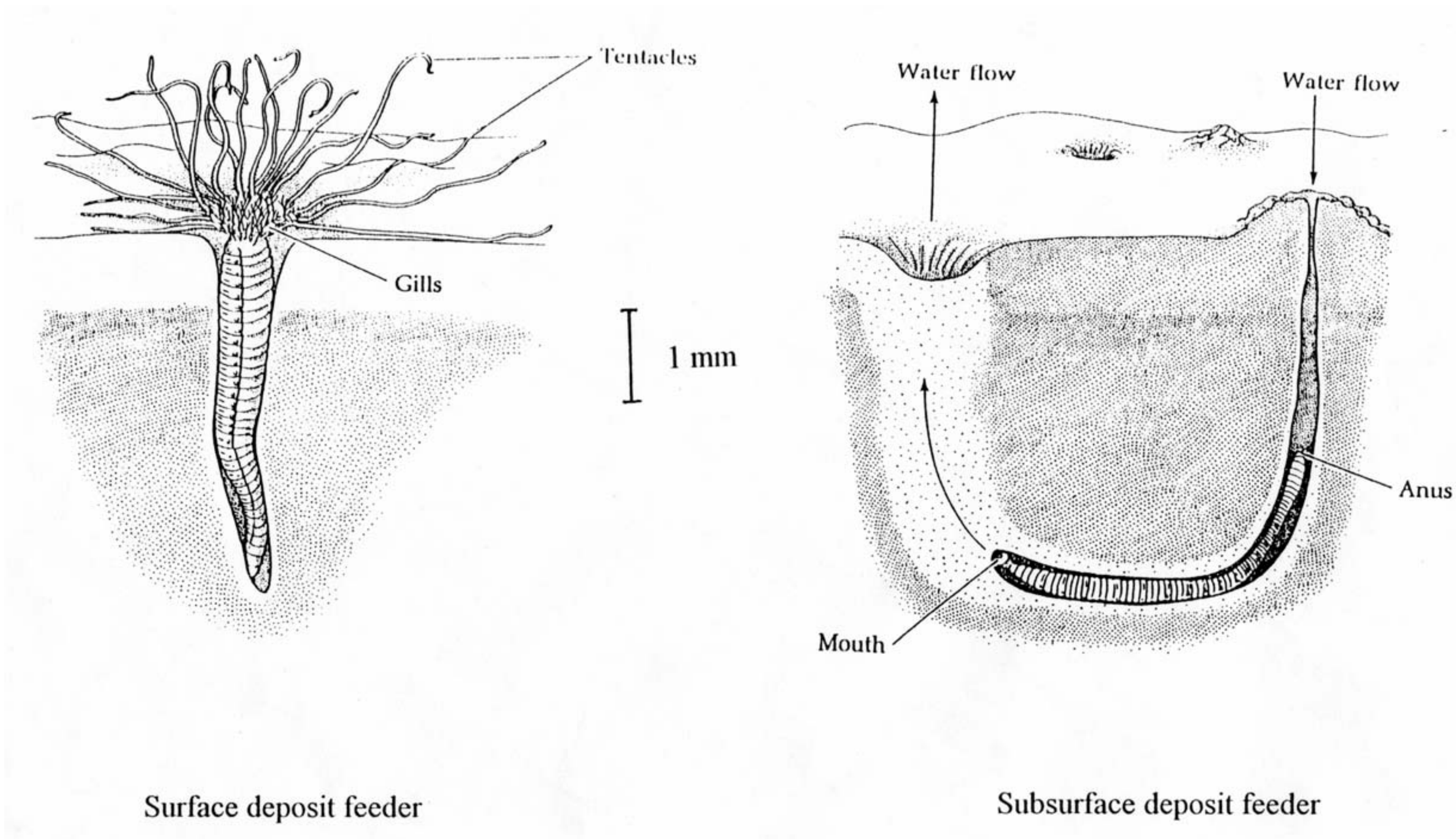

Hyodrothermal Vents discovered on Galapagos Rift in 1977

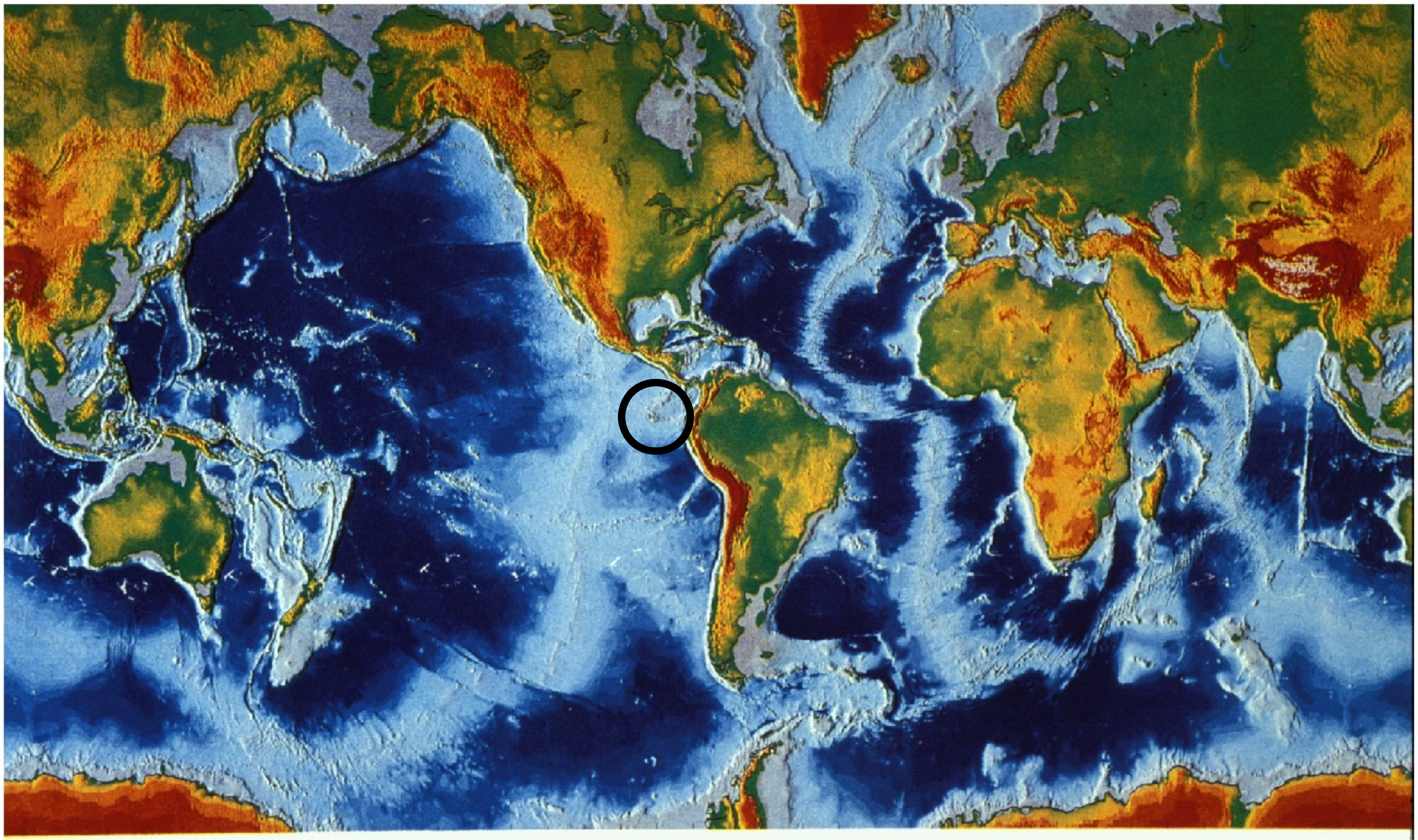

Discovery of hydrothermal vents – Lonsdale 1976 pictures of clams on Axial Ridge of GSC

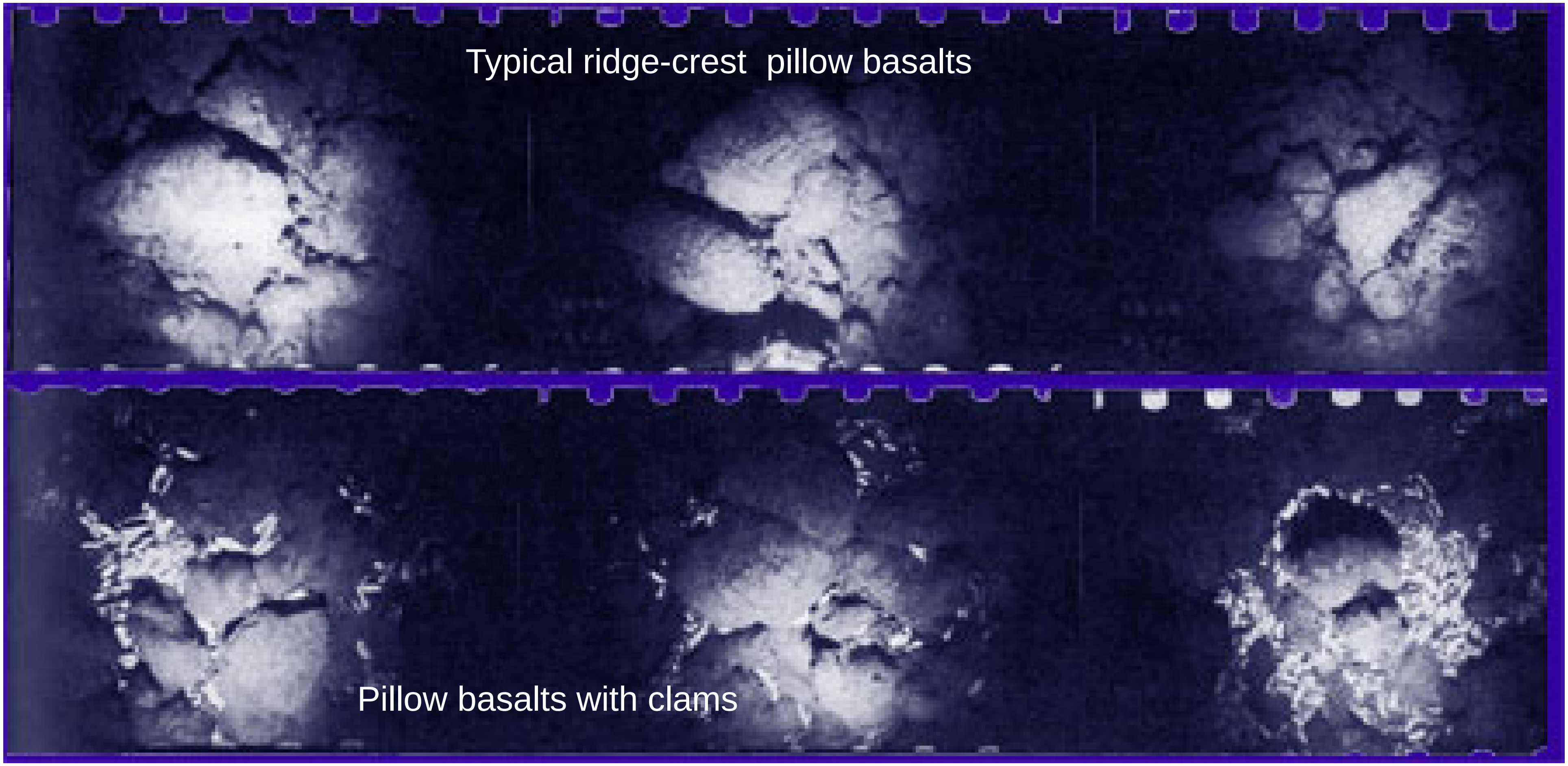

Deep Tow

(SIO)

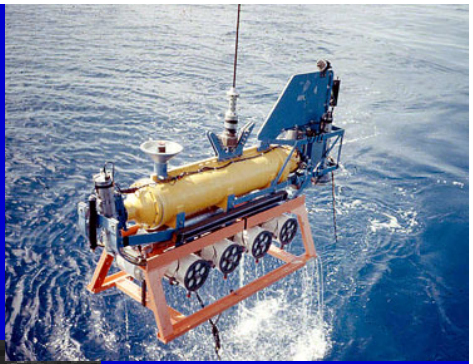

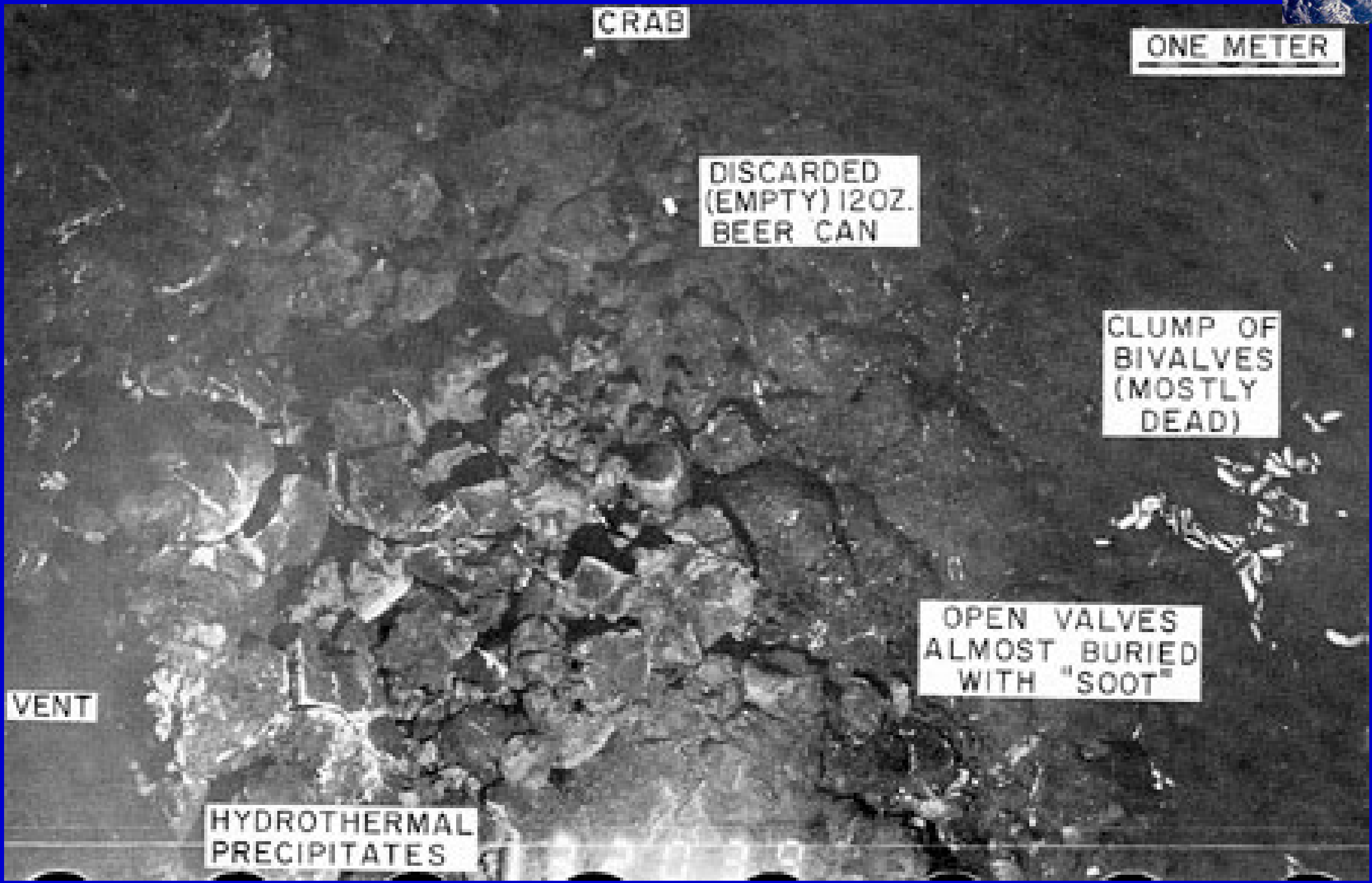

Lonsdale (1977) Clam bake slide

1977 – First Geology Cruise to hydrothermal vent at Galapagos Rift (1979 first Biology Expedition)

As approach vent site, encounter strange biota

Spaghetti worms (enteropneusts)

Galapagos vent periphery

Vesicomyid clams (*Calyptogena magnifica*) at Galapagos vent

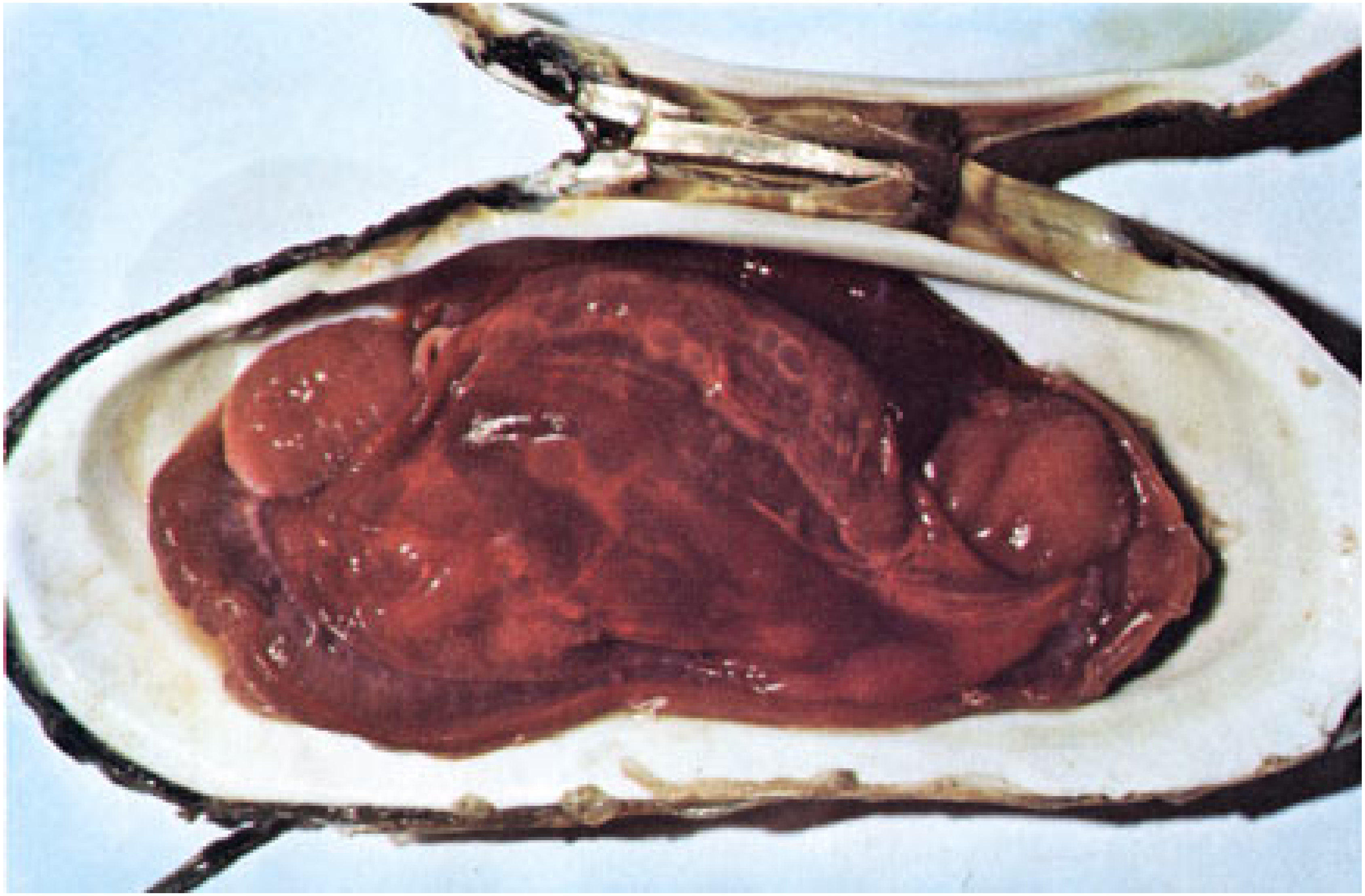

Calyptogena magnifica from Galapagos vent

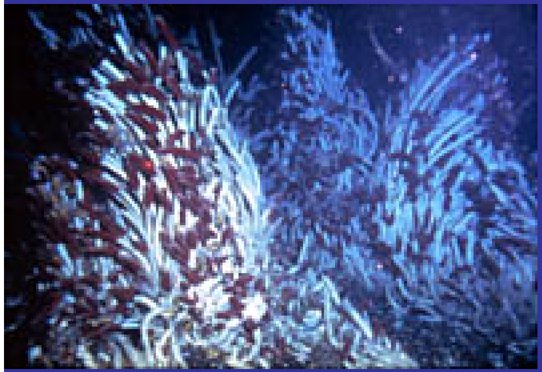

Vestimentiferan worms (*Riftia pachyptila*), limpets and serpulids near vents and in vent throat (low temp.)

Galapagos Rift

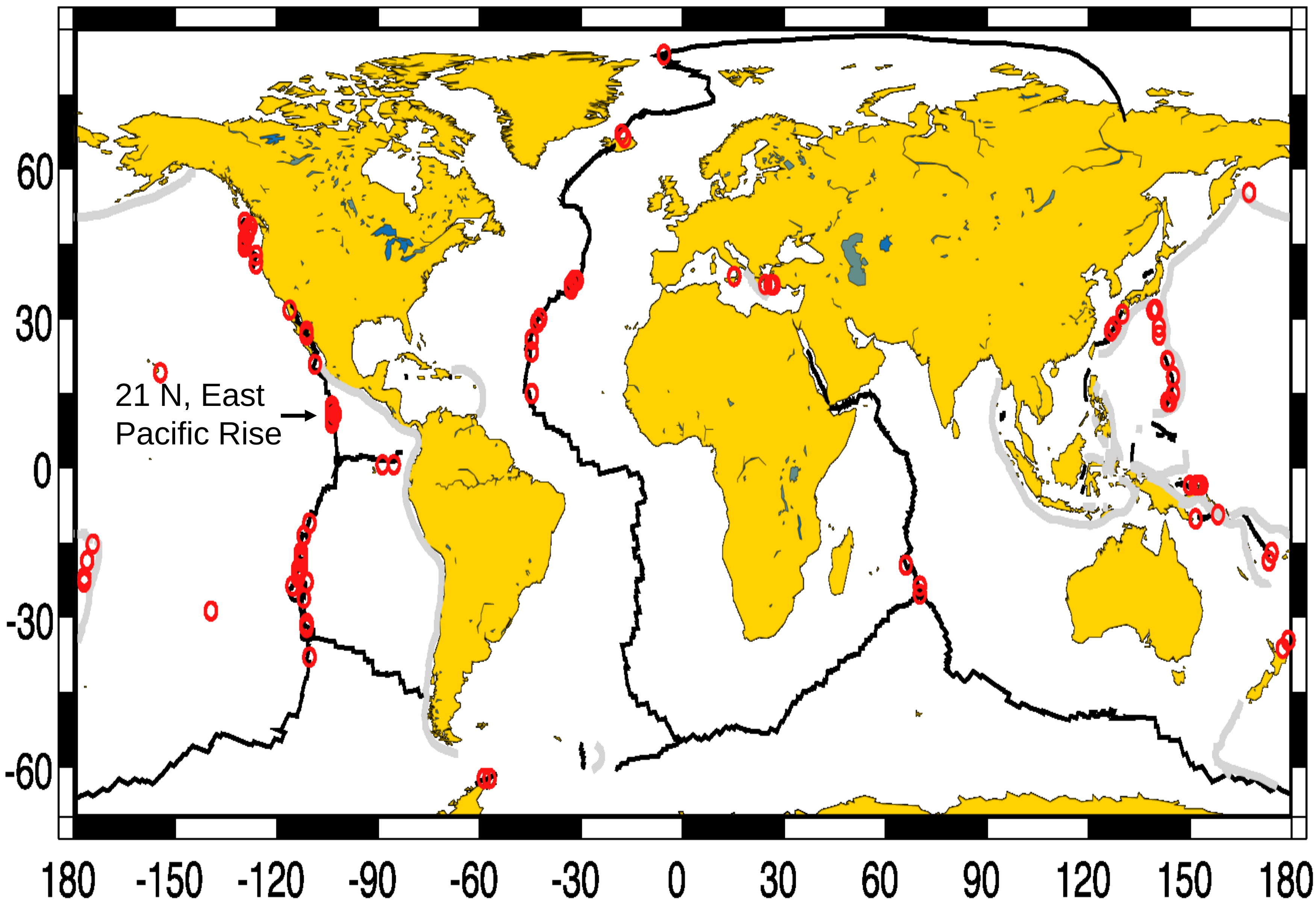
60
30
0
-30
-60
21 N, East
Pacific Rise
180
-150
-120
-90
-60
-30
0
30
60
90
120
150
180

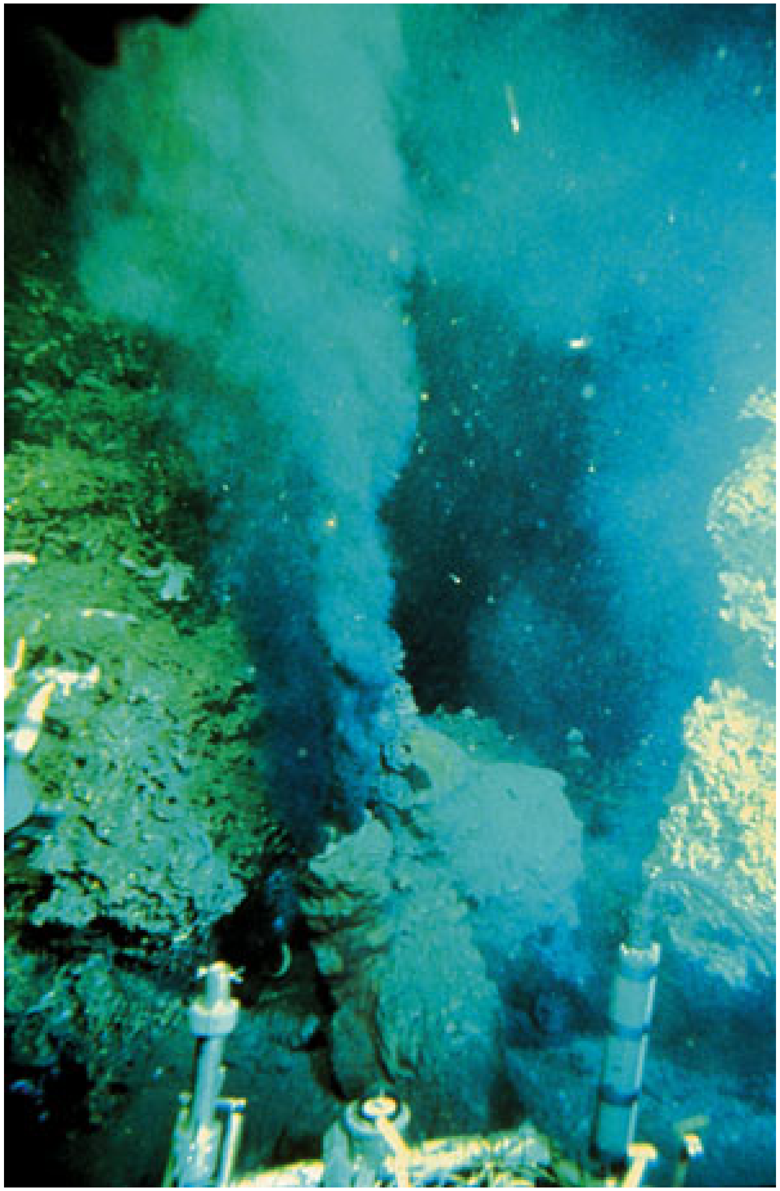

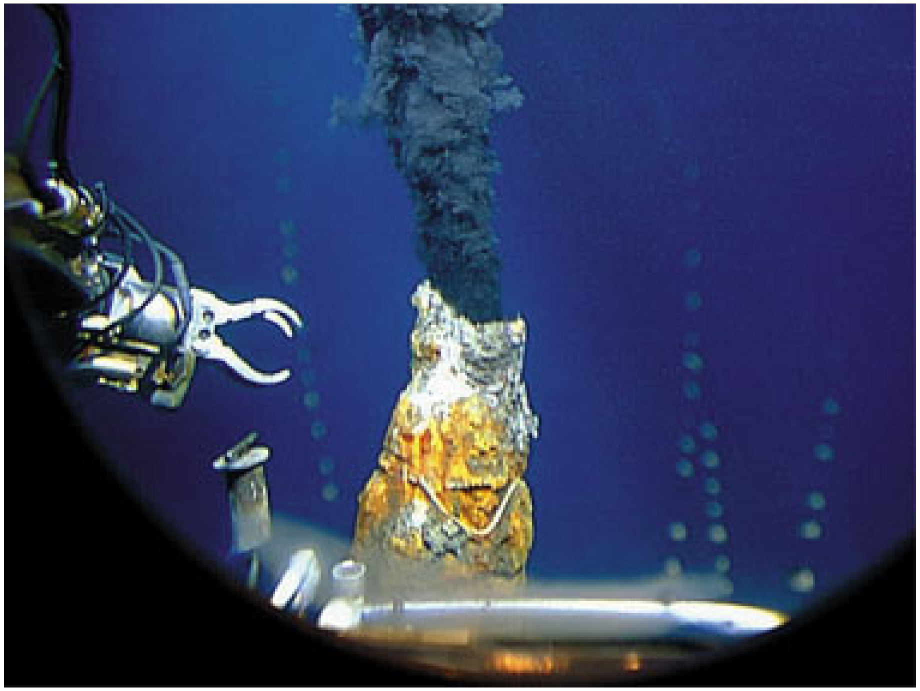

Black smokers

21ºN East Pacific Rise

Chimney formation at hydrothermal vents

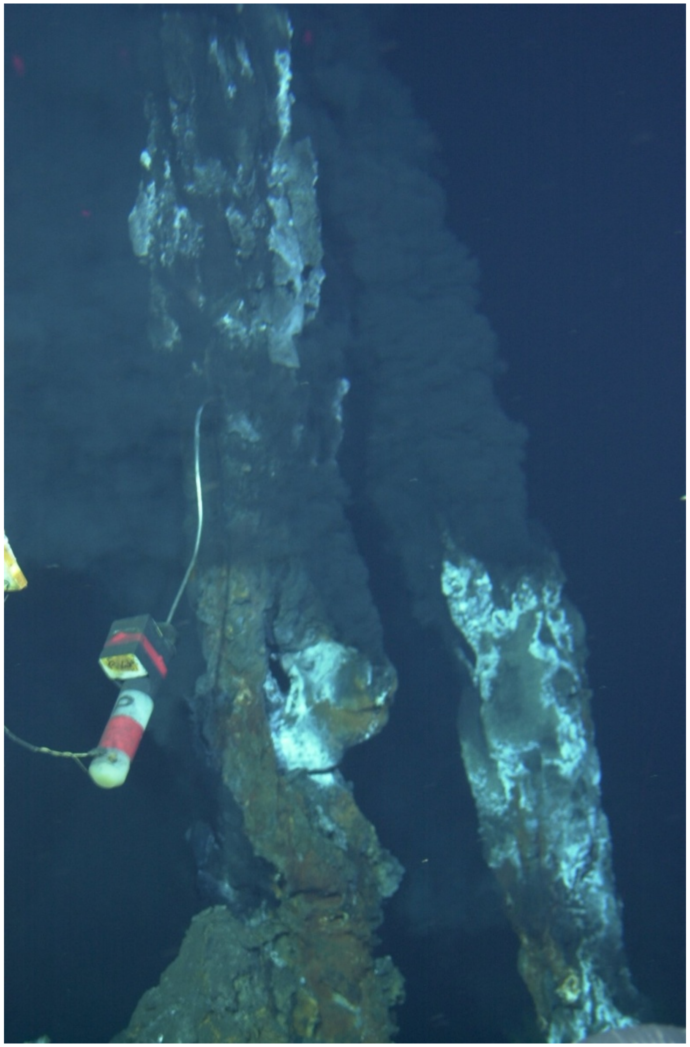

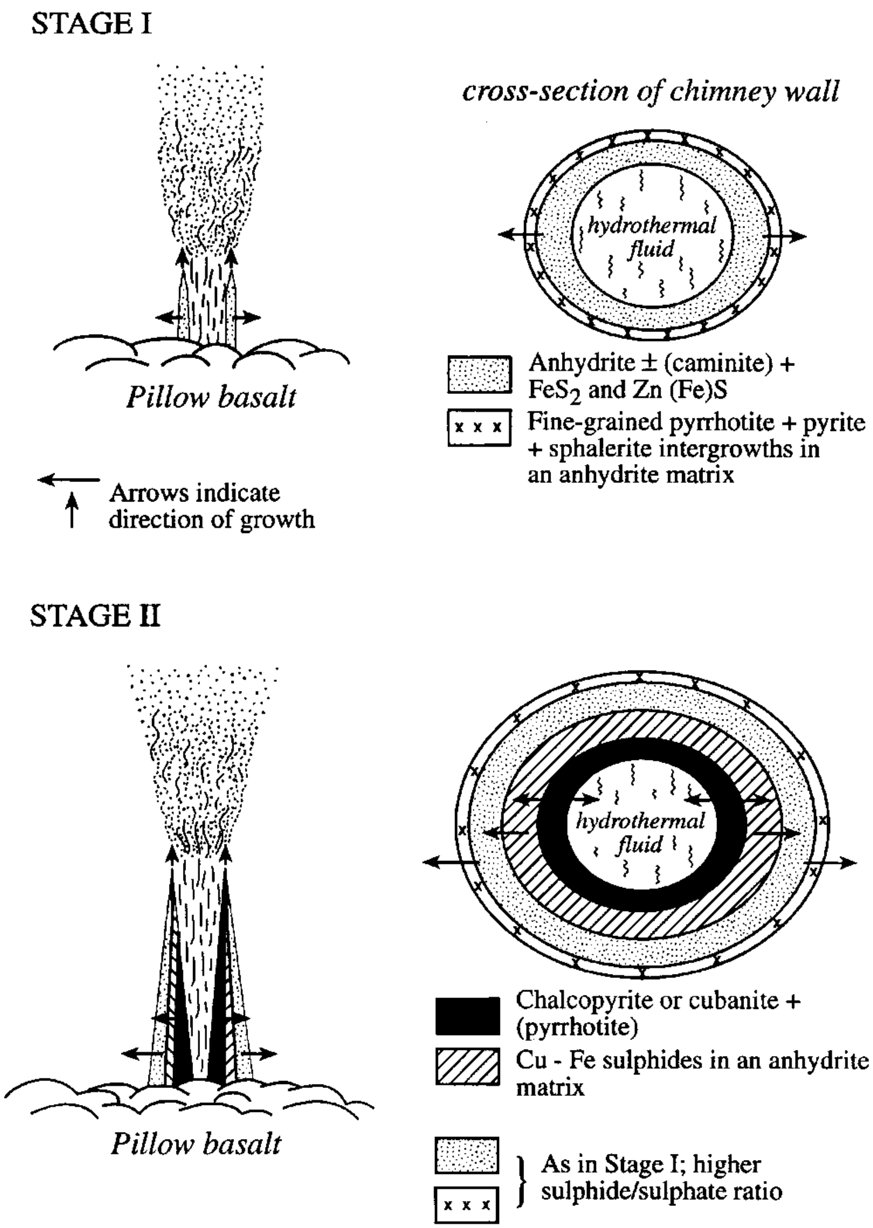

Dominant fauna of the SE Pacific vents

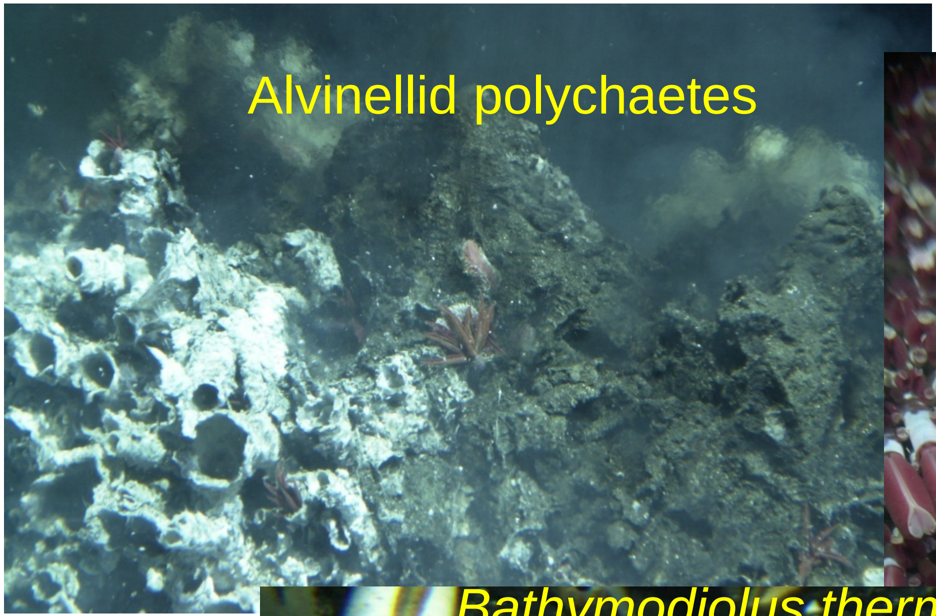

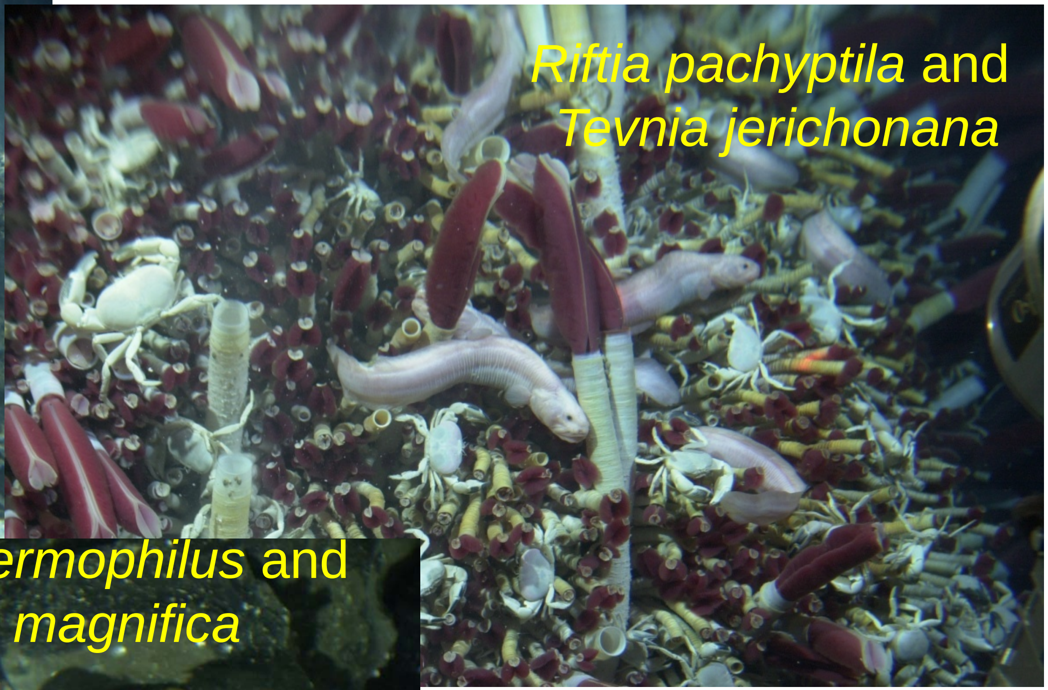

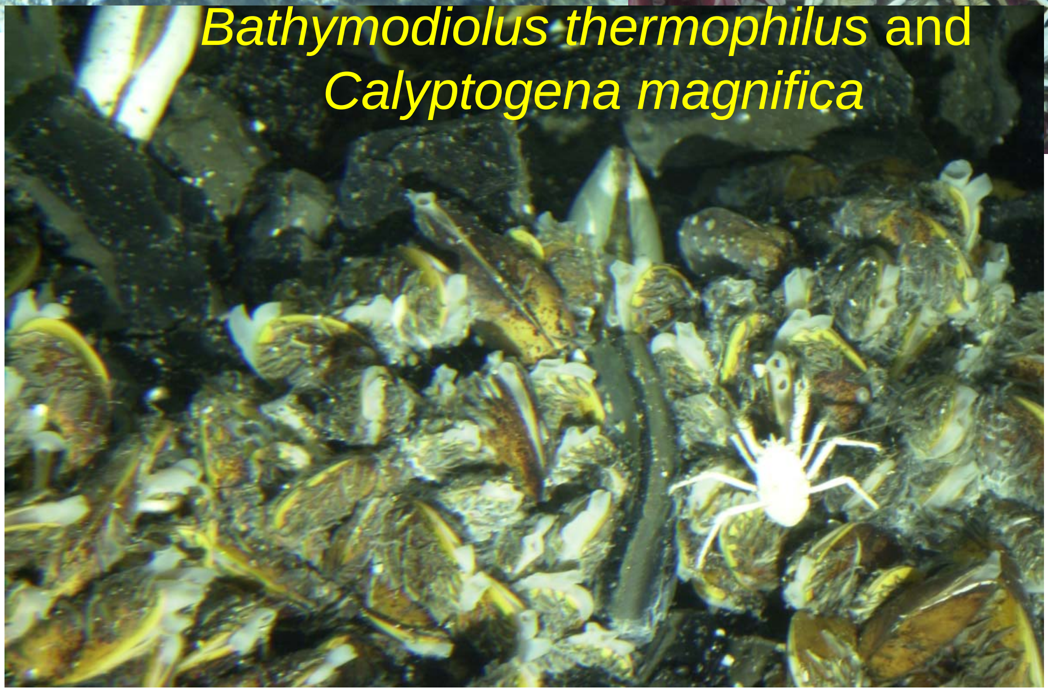

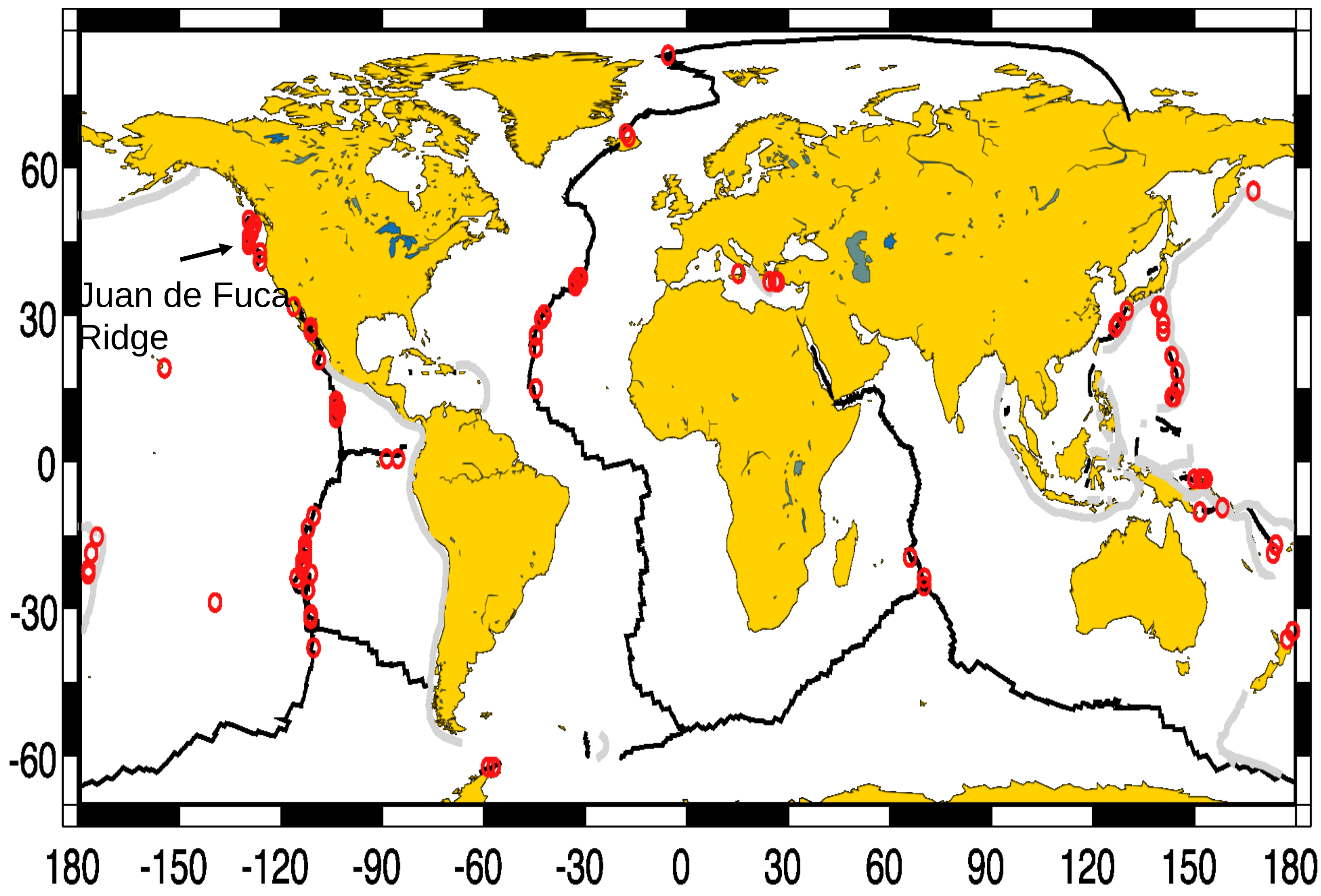
Juan de Fuca
Ridge
60
30
0
-30
-60
180
-150
-120
-90
-60
-30
0
30
60
90
120
150
180

Figure 2.22. "Godzilla," a 45-m-high sulfide mound with flanges on the Juan de Fuca Ridge. The submersible *Alvin* is drawn to scale. From Robigou et al. 1993.

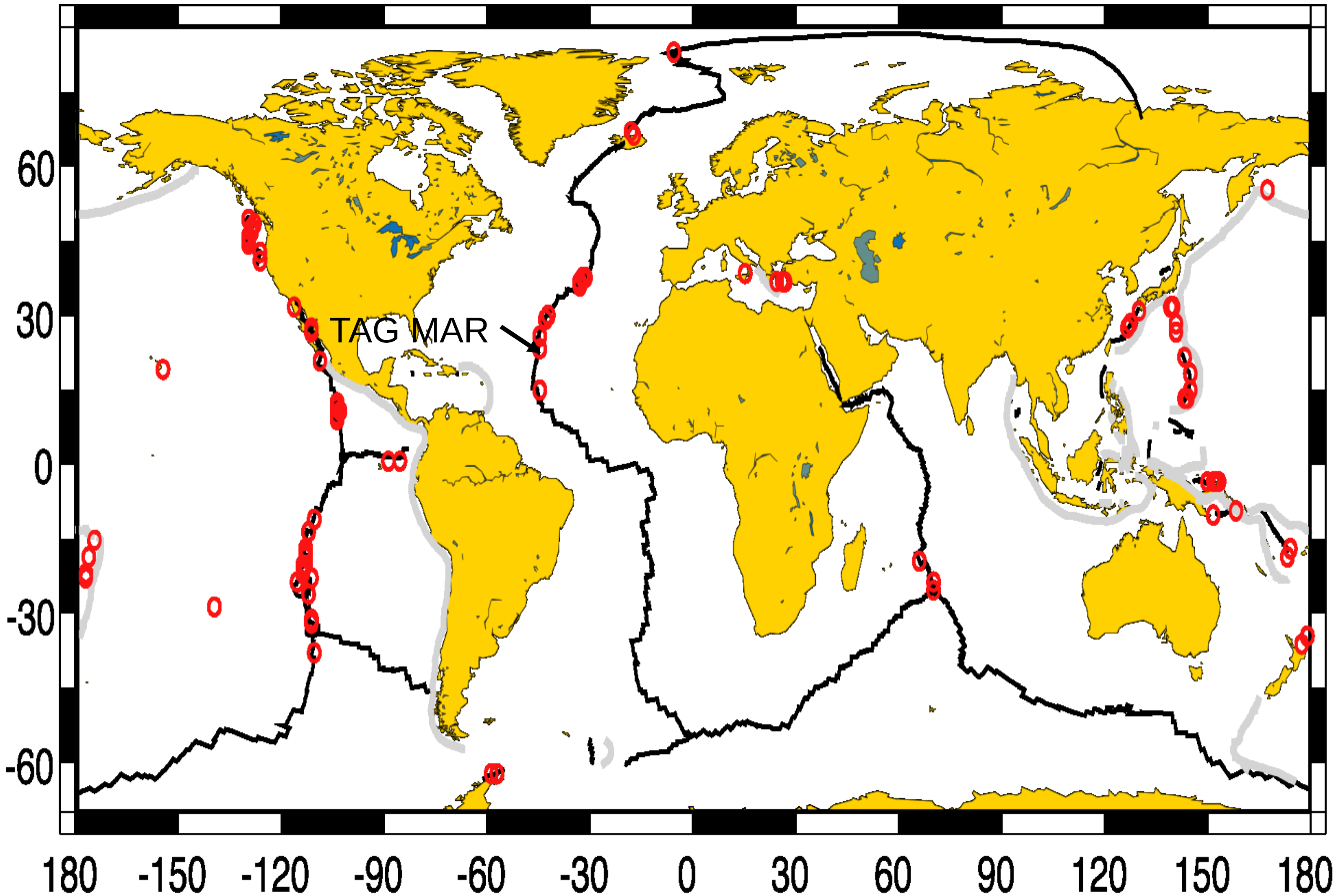

TAG MAR
60
30
0
-30
-60
180
-150
-120
-90
-60
-30
0
30
60
90
120
150
180

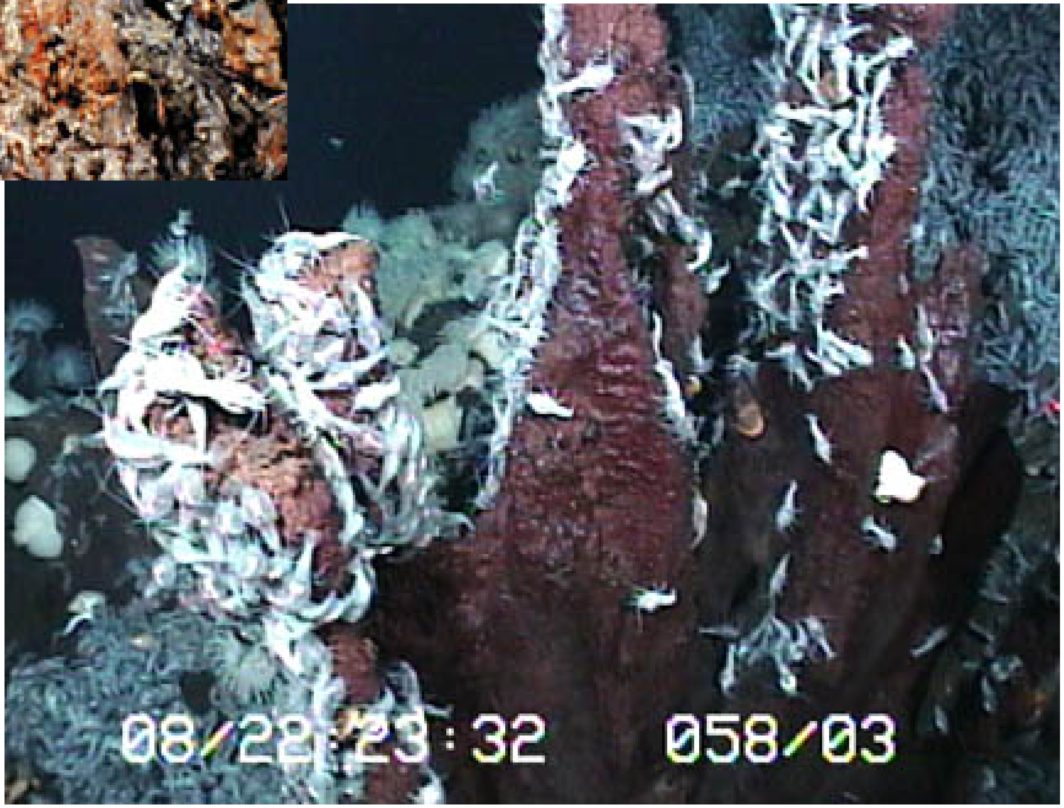

Mussels and vent shrimp (*Rimicaris exoculata*) at Mid-Atlantic Ridge sites

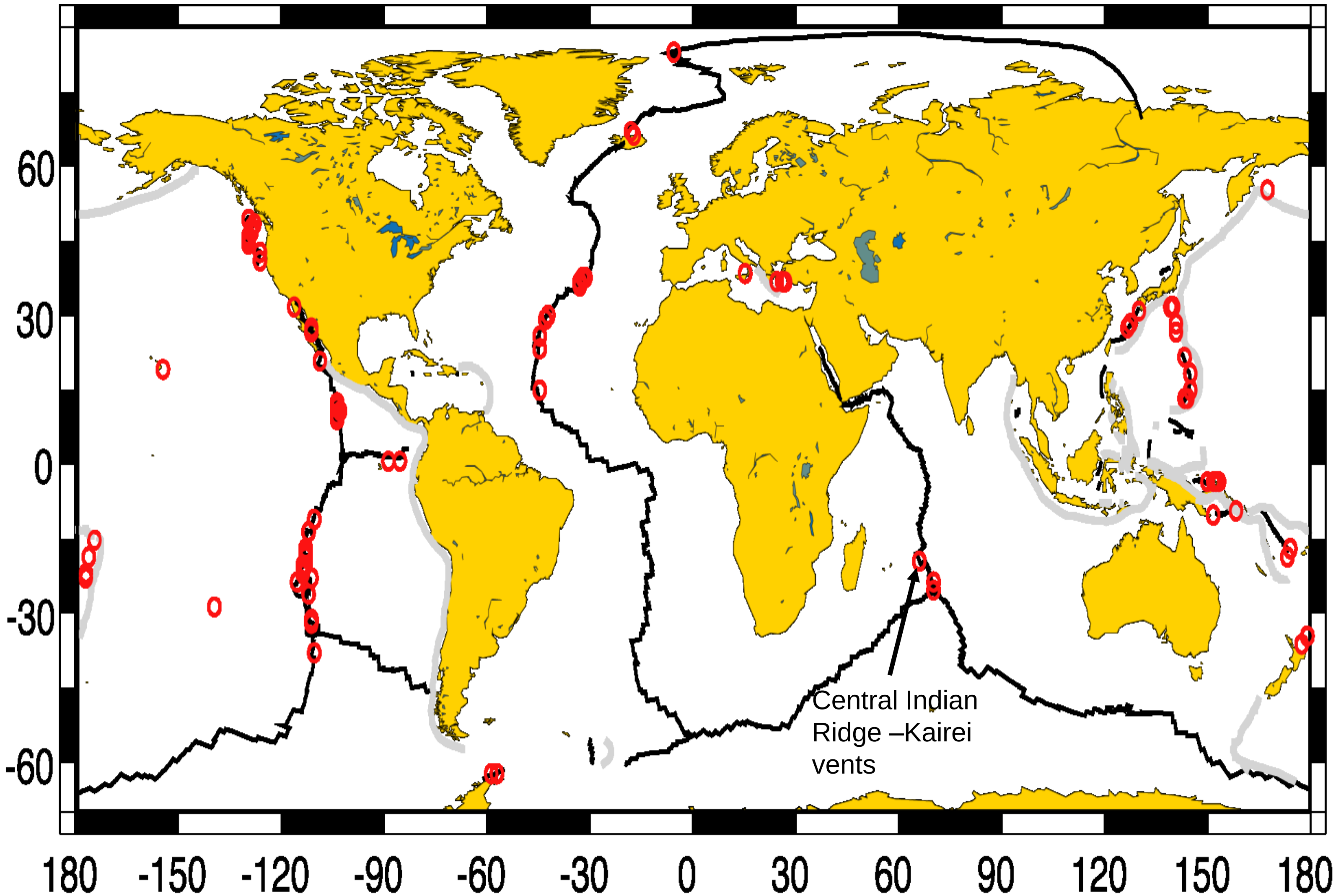
60
30
0
-30
-60
180
-150
-120
-90
-60
-30
0
30
60
90
120
150
180
Central Indian
Ridge –Kairei
vents

And what's in the Indian Ocean?

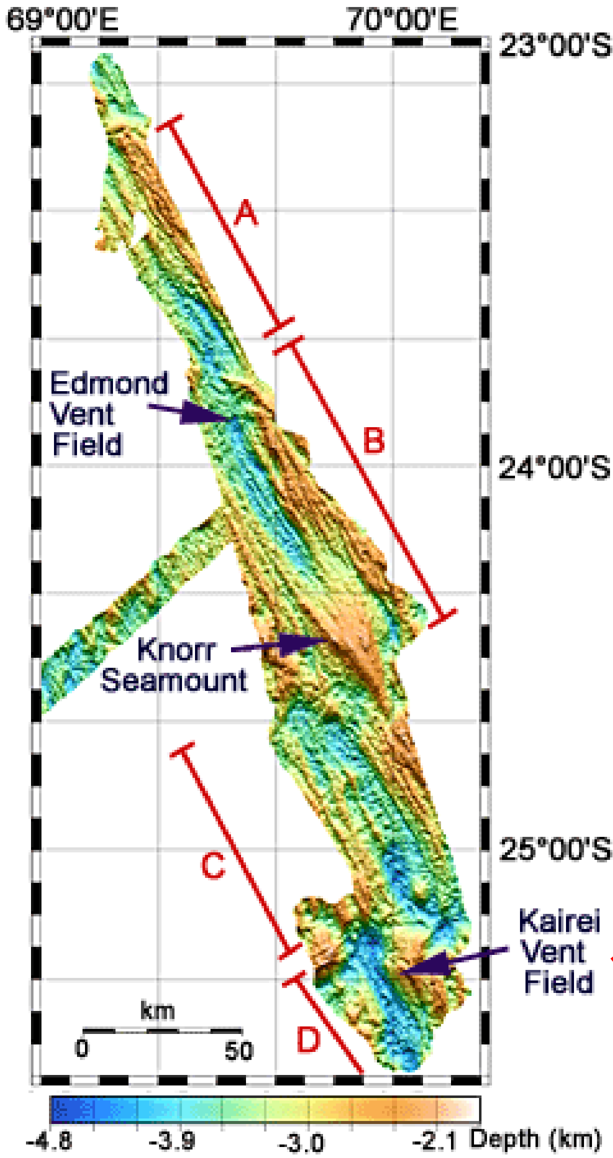

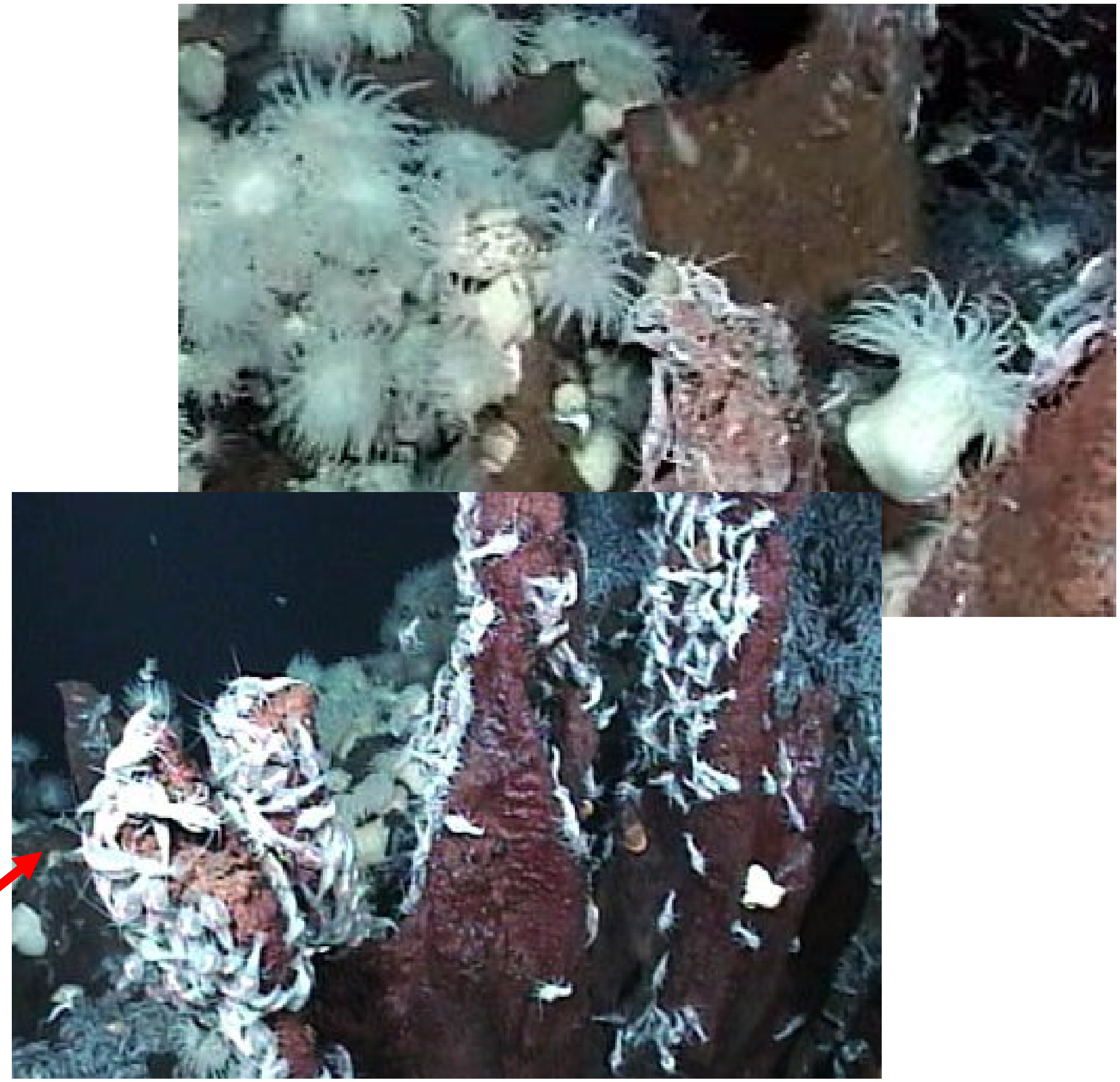

Known vent-sites (Baker & German, 2004)

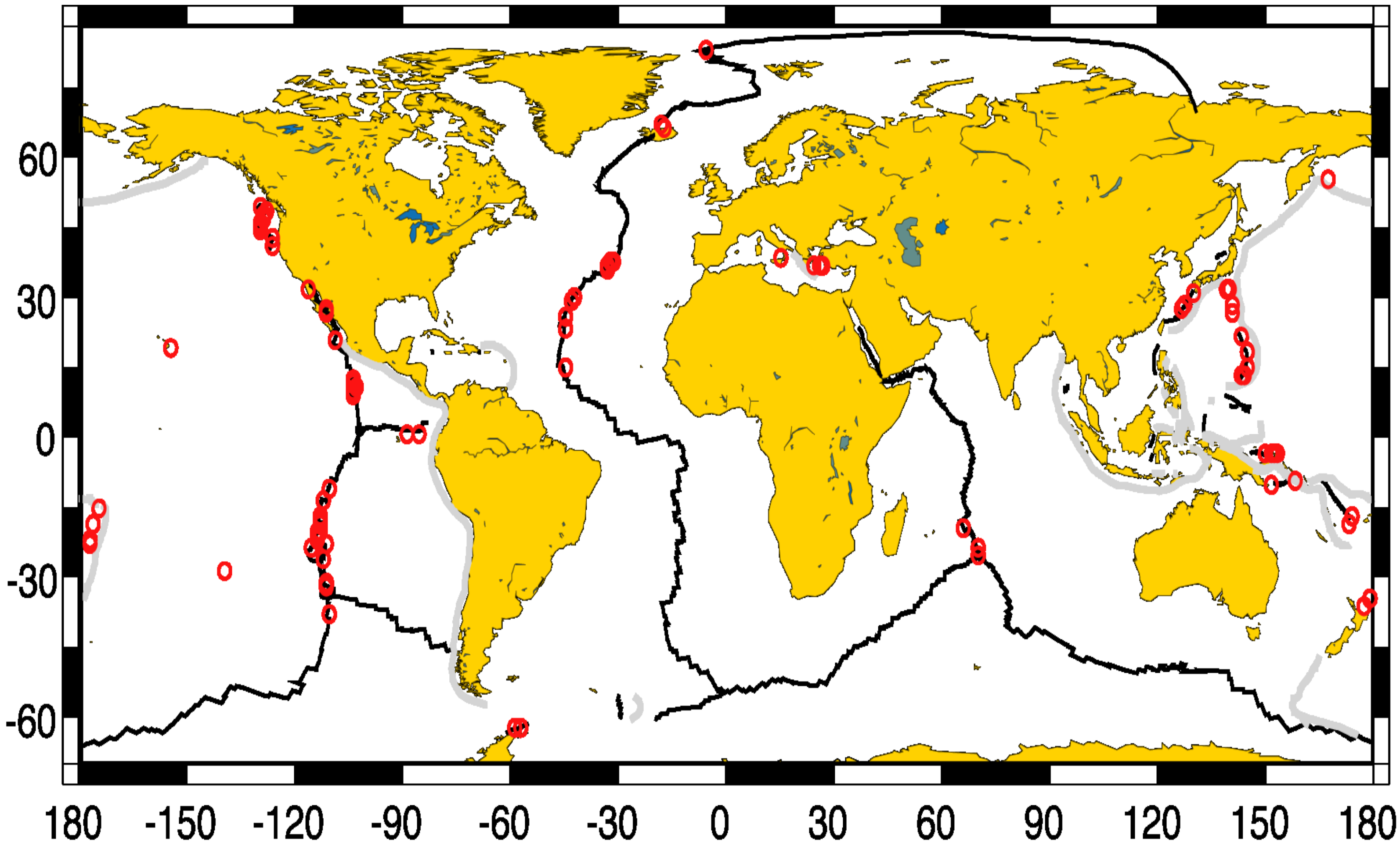

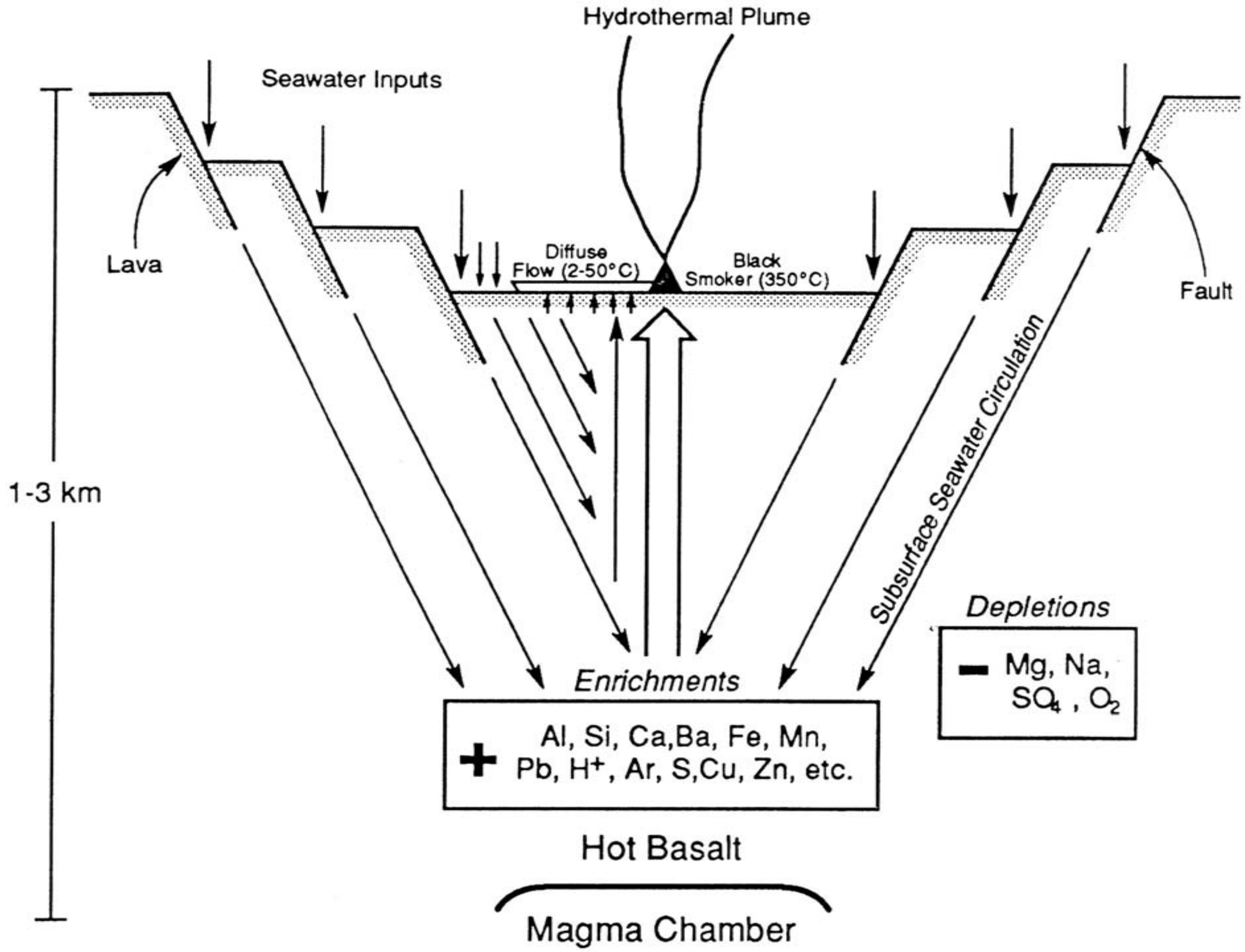

Fig. 1. Formation of hydrothermal vents on the sea floor takes place at seafloor spreading centers. Cracks and faults allow sea water to penetrate the sea floor and react with hot basalt at great depths. The chemically modified water rises up to the sea floor to form hydrothermal vents. Typical enrichments and depletions of vent water are illustrated here, but regional and local differences in temperature and pressure of reaction and water-to-rock ratios can introduce significant geochemical variations[11] that may influence the biota. In a few areas, where oceanic spreading centers are overlain by pelagic or terrigenous sediments, reaction of the hot sea water with sediment on its transit to the sea floor can generate more exotic vent-water chemistries, including enrichment in hydrocarbon content due to cracking of recent organic carbon in the sediment cover. Guaymas Basin, in the Gulf of California, is a good example of a vent field overlain by sediment[6].

Van Dover, 1990

TABLE 5 The "Metabolic Menu" of Potential e⁻ Donors, e⁻ Acceptors, and C Sources for Bacterial Growth at Selected Deep-Sea Hydrothermal Vents

	H_2S (mmol/kg)	H_2 (mmol/kg)	CH_4 (mmol/kg)	CO_2 (mmol/kg)	Fe (µmol/kg)	Mn (µmol/kg)	NH_4^+ (µmol/kg)	$[NO_3^-–NO_2^-]$ (µmol/kg)
Galapagos Rift[a] (5°–13°C)	0.05–0.12	<0.001	0.003–0.009	—[b]	0.1–10	10–35	—	0–10
21°N East Pacific Rise[c] (>300°C)	4–9	0.36–1.7	0.06–0.09	5.7	750–2,500	700–1,000	<1	—
13°N East Pacific Rise[d] (350°C)	—	4.1–5.6	0.03–0.06	10.8–16.7	—	—	—	—
Juan de Fuca Ridge[e] (29°C)	0.33	—	—	40	2.6	27.7	—	—
Juan de Fuca Ridge[f] (328°C)	7.1	—	0.025	50	1,065	1,150	—	—
Endeavour Ridge[g] (>350°C)	—	0.025–0.075	0.5–1.4	5–11	—	—	600	—
Explorer Ridge[h] (276°–306°C)	0.7–0.9	—	—	—	0.006–0.020	—	18,000–20,000	26–32
S. Juan de Fuca[i] (>350°C)	3–4.4	0.27–0.53	0.08–0.12	3.9–4.5	10,300–17,800	2,600–4,480	—	—
Juan de Fuca[j] Cl⁻ enriched (150°–328°C)	7	—	—	—	1,071	1,133	—	—
Juan de Fuca[j] Cl⁻ depleted (5°–299°C)	—	—	—	—	9	162	—	—
Guaymas Basin[k]	3.8–6	1–5	2–7	16–24	17–180	128–236	10,000–16,000	—
Loihi Seamount[l] (10°–30°C)	<0.002	<0.01	0.007	300–418	1,010–1,460	21–48	5–7	0–10
23°N Mid-Atlantic Ridge[m] (335°–350°C)	2.7–5.9	—	0.06	—	1,800–2,121	443–491	—	—
Lau Basin[n] (334°C)	—	—	—	—	1,200–2,900	5,800–7,100	—	—

Karl, D. 1995. *The Microbiology of Deep-Sea Hydrothermal Vents,* edited by D. Karl, CRC press, 299 pp.

TABLE 5.1.
Classification of major physiological groups of bacteria on the basis of electron donors and major carbon sources used in metabolism

Type of Metabolism	*Carbon Source*	*Electron Donor*
Phototrophy[a]		
Photoautolithotroph	CO_2	H_2O, H_2S, S^0, H_2
Photoheterolithotroph	organic substrate	H_2O, H_2S, S^0, H_2
Photoautoorganotroph	CO_2	organic substrate
Photoheteroorganotroph	organic substrate	organic substrate
Photomixotroph[b]	mixed: CO_2 and organic	mixed: inorganic and organic
Chemotrophy[c]		
Chemoautolithotroph	CO_2	reduced inorganic substrate (e.g., H_2, H_2S, $S_2O_3^{2-}$, S^0, NH_4^+, Fe^{2+})
Chemoheterolithotroph	organic substrate	reduced inorganic substrate (e.g., H_2, H_2S, $S_2O_3^{2-}$ S^0, NH_4^+, Fe^{2+})
Chemoautoorganotroph	CO_2	organic substrate
Chemoheteroorganotroph	organic substrate	organic substrate
Chemomixotroph[d]	mixed: CO_2 and organic	mixed: inorganic and organic

From Karl 1995.

TABLE 2 Potential Bacterial Metabolic Processes at Deep-Sea Hydrothermal Vents

Conditions	Electron (energy) donor	Electron acceptor	C source	Metabolic process
Aerobic	H_2	O_2	CO_2	H oxidation
	HS^-, S^o, $S_2O_3^{2-}$, $S_4O_6^{2-}$	O_2	CO_2	S oxidation
	Fe^{2+}	O_2	CO_2	Fe oxidation
	Mn^{2+}	O_2	?	Mn oxidation
	NH_4^+, NO_2^-	O_2	CO_2	Nitrification
	CH_4 (and other C-1 compounds)	O_2	CH_4, CO_2, CO	Methane (C-1) oxidation
	Organic compounds	O_2	Organic compounds	Heterotrophic metabolism
Anaerobic	H_2	NO_3^-	CO_2	H oxidation
	H_2	S^o, SO_4^{2-}	CO_2	S and sulfate reduction
	H_2	CO_2	CO_2	Methanogenesis
	CH_4	SO_4	?	Methane oxidation
	Organic compounds	NO_3^-	Organic compounds	Denitrification
	Organic compounds	S^o, SO_4^{2-}	Organic compounds	S and sulfate reduction
	Organic compounds	Organic compounds	Organic compounds	Fermentation

Adapted from Karl (1987).

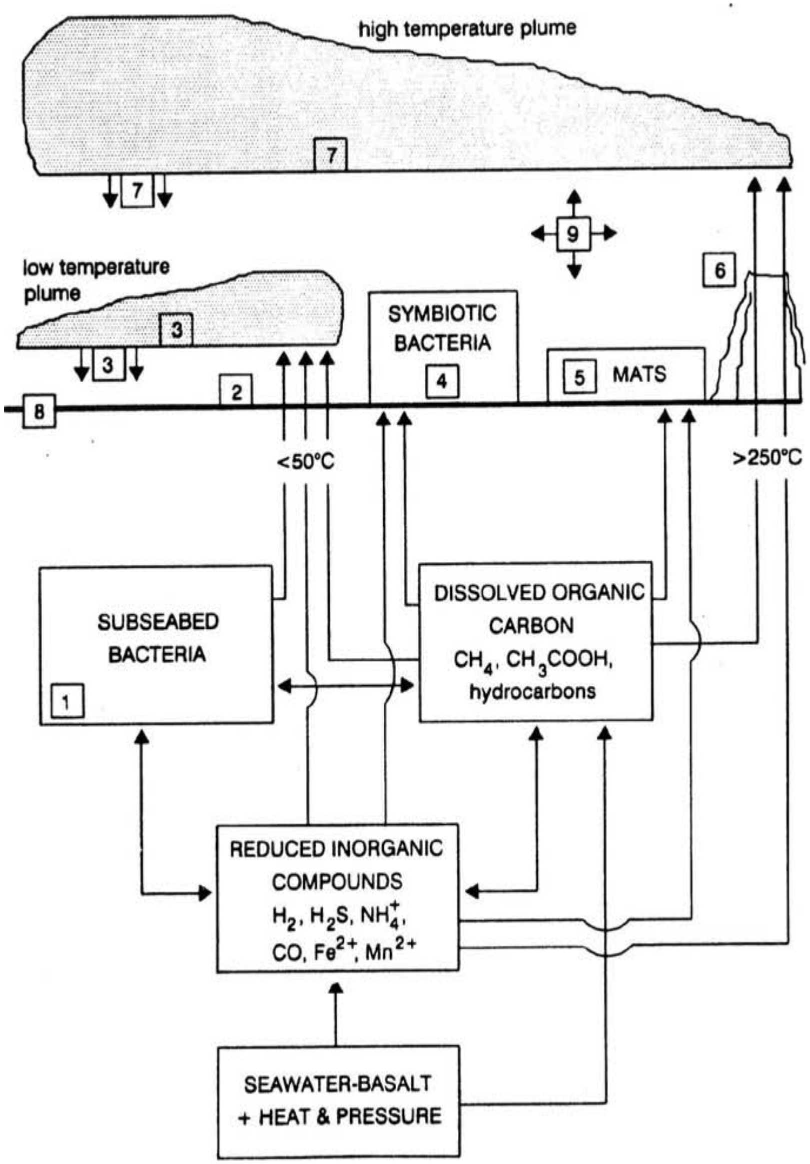

FIGURE 8 The various potential productivity loci and regions of bacterial biomass accumulations in a typical hydrothermal vent ecosystem. (See text for more details of these habitats and populations.) 1, Attached bacterial production in the subseabed habitat. The biomass produced in these heated, anoxic regions of the hydrothermal system is probably unavailable for direct consumption by macrofauna until dislodged and transported upward by the flowing hydrothermal fluids. Both reduced inorganic and reduced organic sources of C and energy are available to these bacterial assemblages, but the absence of certain electron acceptors (e.g., O_2 and NO_3^-) probably limits the spectrum of metabolic pathways. The dislodged organic particles emitted at the vent orifice are typically clumps of cells (>12 μm) which can be consumed directly by suspension-feeding macrofauna. 2, Bacterial production by organisms growing attached to rocks or animal surfaces exposed to the discharged vent waters in the region of turbulent mixing with ambient deep-sea waters. This habitat is the most conducive for the chemolithoautotrophic production of organic matter because of access to both reduced inorganic substrates from below and dissolved O_2 from bottom-water entrainment. Grazers actively consume these attached bacterial assemblages. 3, Bacterial biomass transport by, production in, and export from the near-field, low-temperature vent plumes. This habitat includes the passive "fallout" zone and the active regions of particle resuspension by bottom currents and animal movements. The availability of organic matter in this habitat decreases with distance from the vent site. These bacterial populations are a complex mixture of cells originally derived from the subseabed habitat, the vent orifice, and entrained deep seawaters. Only the latter communities are likely to be metabolically responsive to the vent-derived nutrients in these diluted plumes because of low-temperature inhibition of the true vent bacteria. The organic fallout from these plumes provides a source of C and energy for zooplankton and to the near-field benthic communities. 4, Ecto- and endosymbiotic bacteria living with numerous invertebrate hosts. Many of these symbiotic associations undoubtedly provide a nutritional benefit for the host, the symbiont, or both; however, the quantitative relationships and the precise pathways of C and energy flow are poorly known. 5, Bacterial production and, occasionally, massive biomass accumulations at the seawater–sediment interface of regions exposed to vent fluid flow. The extensive bacterial mats may exist because of limited grazing pressure rather than high production rates. 6, Bacterial production in and around the high-temperature "black smoker" chimney habitat. These specialized and extreme habitats may support the hyperthermophiles, which have been isolated from deep-sea vents, and the hypothesized "phototrophic" vent bacteria. The bacteria growing attached to the mineralized smoker chimneys can be grazed directly by vent macrofauna. 7, Bacterial biomass transport by, production in, and export from far-field, high-temperature hydrothermal plumes. This vent habitat can extend for hundreds of kilometers from the discharge site. The nutrient-responsive populations are most likely the ambient deep water bacterial cells that are entrained by turbulent mixing. The temperature of the hydrothermal plume (1° to 3°C) relative to the source fluids (>250°C) suggests that most vent-derived bacteria are low-temperature inactivated. Both zooplankton and far-field benthic communities benefit from these bacterial production processes. 8, Bacterial production in the sediment habitats of ridge flanks extending out 10 to 100 km from the ridge crest. These extensive habitats actually may be the most important sources of bacterial C production in the vent ecosystem, but quantitative studies have not been conducted. This hypothesized production could fuel a specialized benthic food web, or could simply be a metabolic sink for hydrothermal energy. 9, Secondary bacterial production by decomposer populations present throughout the hydrothermal vent ecosystem. The export of organic matter by the high-temperature hydrothermal plumes and by mobile predators can extend the influence of the vent into regions well beyond the localized vent field per se.

Karl, D. 1995. *The Microbiology of Deep-Sea Hydrothermal Vents,* edited by D. Karl, CRC press, 299 pp.

Typical Deep-Sea Floor (2500 m North Carolina slope)

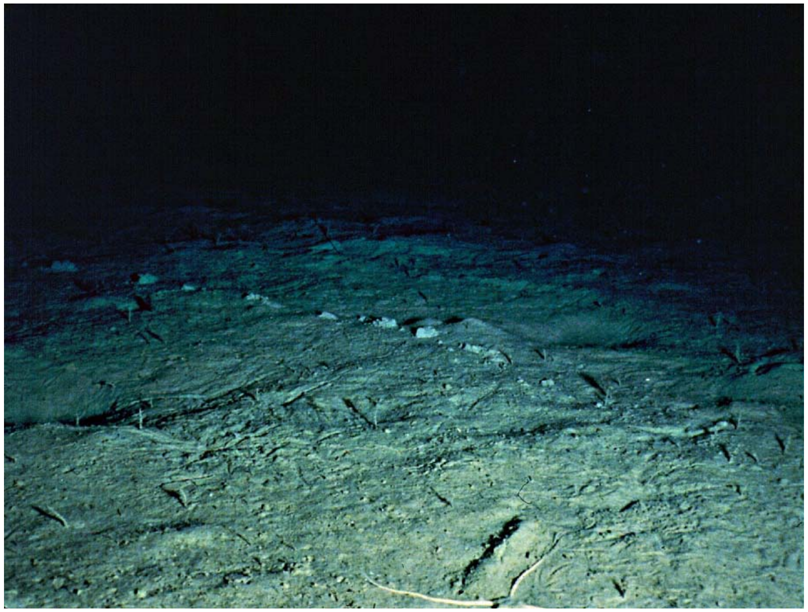

~ 1 g/m^2 of biomass

van Dover 2000

Hydrothermal Vent (EPR)

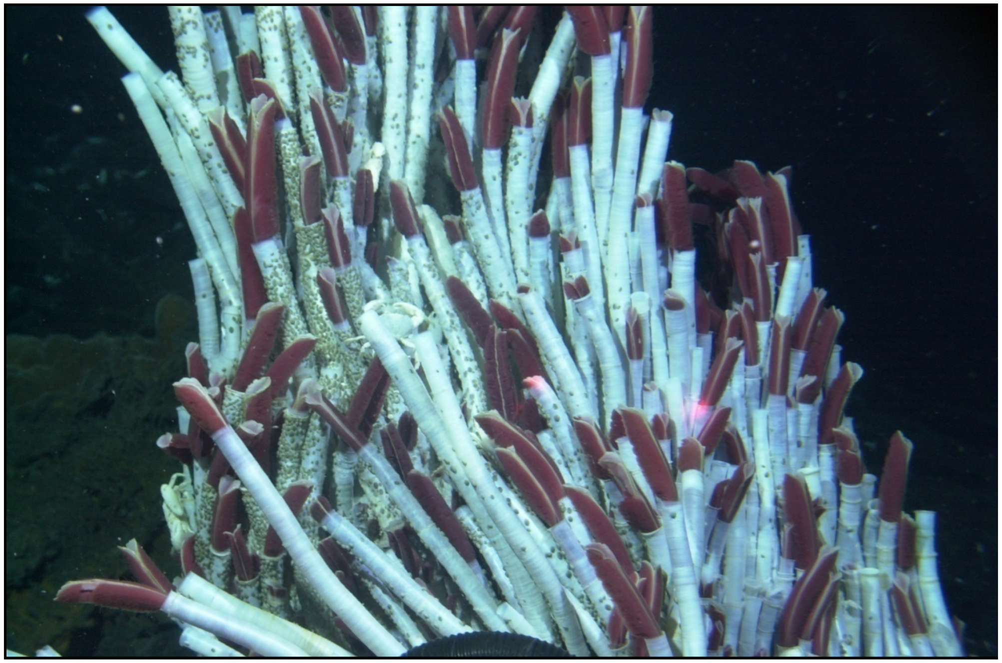

2-meter long tube worms

> 10 kg/m^2 of biomass

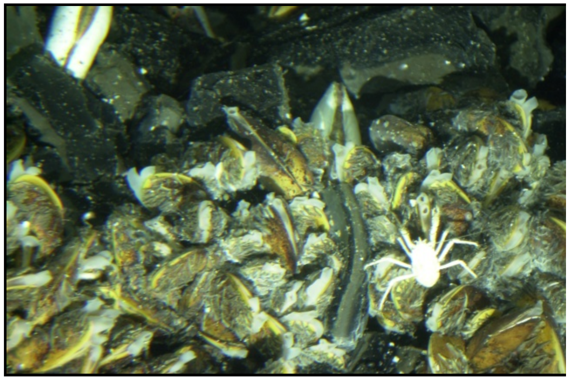

30-cm clams and mussels

VERENA TUNNICLIFFE ,1991

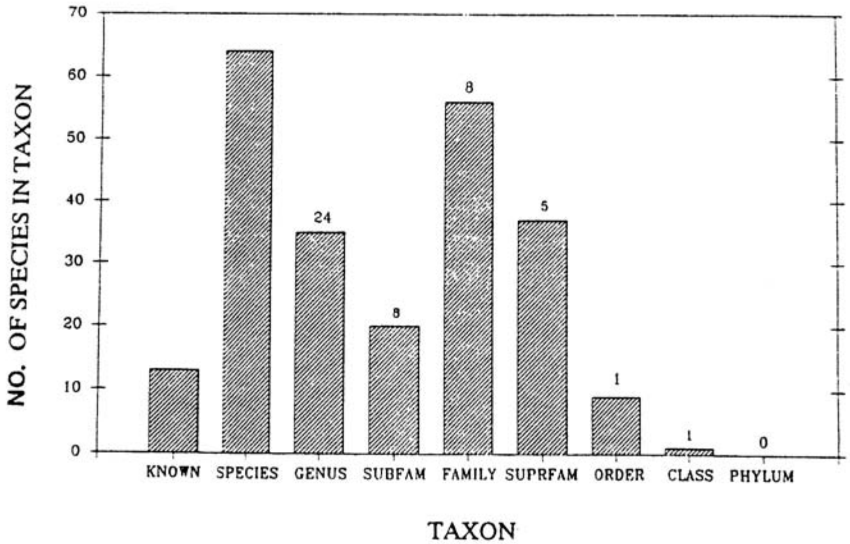

Fig 12.—Distribution of taxonomic levels at which vent species are new science. Of the 236 species listed in Table II (p. 344), 13 are known habitats other than vents. There are 63 new species in genera knov elsewhere, 35 species in 24 new genera, 20 species in 8 new subfamilies, et

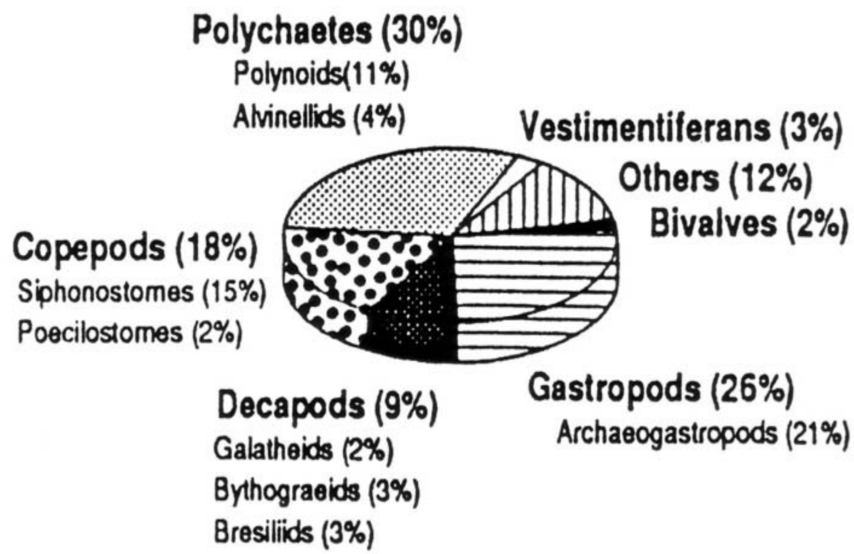

Fig. 4. Species representation of major taxonomic groups in the combined vent fauna of Mid-Atlantic Ridge, East Pacific Rise, Juan de Fuca, Explorer and Mariana vent sites. The total number of species is 193.

Van Dover, 1990

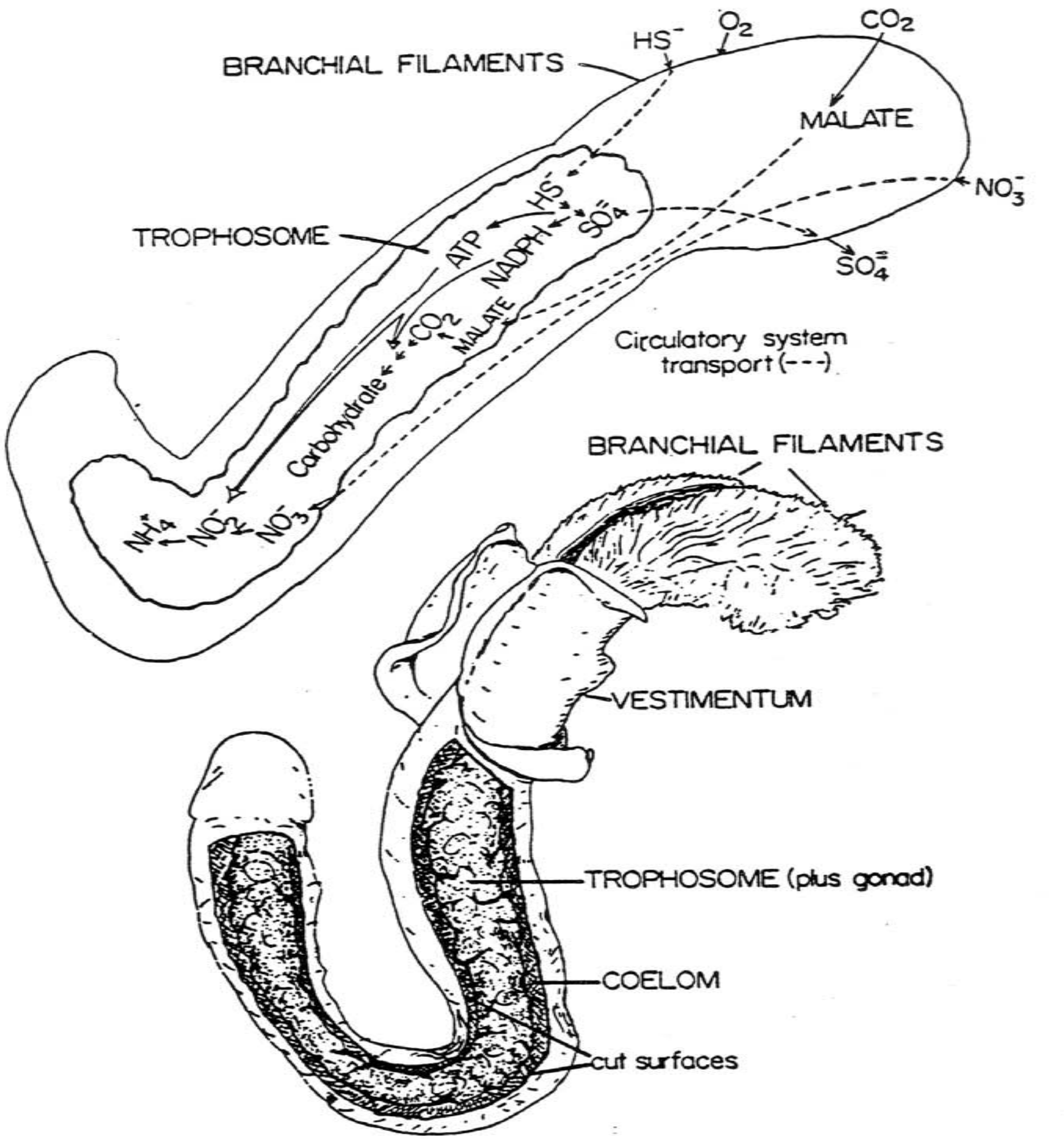

Fig. 1. Drawings to show anatomical plan (lower) and proposed biochemical organization of symbiosis (upper) in *Riftia pachyptila*; proposed transformations in carbon, sulfur, and nitrogen metabolism occurring in symbiosis are indicated; see text for details of metabolic organization; from Felbeck and Somero (1982).

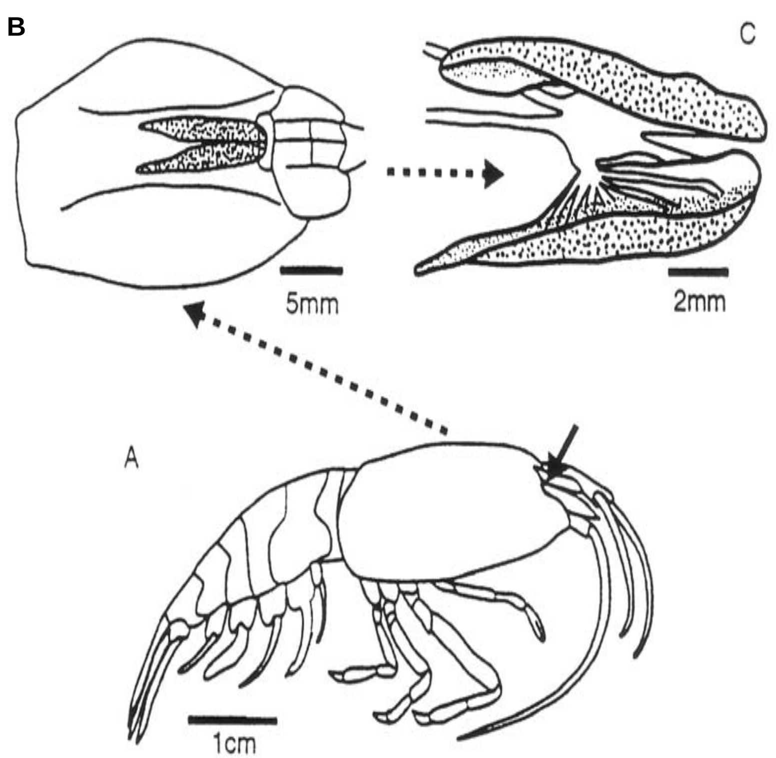

Figure 7.22. A. Lateral view of *Rimicaris exoculata*. Note the lack of eyestalks and conventional compound eyes (arrow). B. Oblique dorsal view showing the location of the dorsal eye (stippled area) underlying the thin transparent carapace. C. Dissection of the dorsal eye. The fused anterior tips have been separated to reveal the underlying connections to the brain (supraesophageal ganglion) of the shrimp. From Van Dover et al. 1989.

Van Dover, 2000

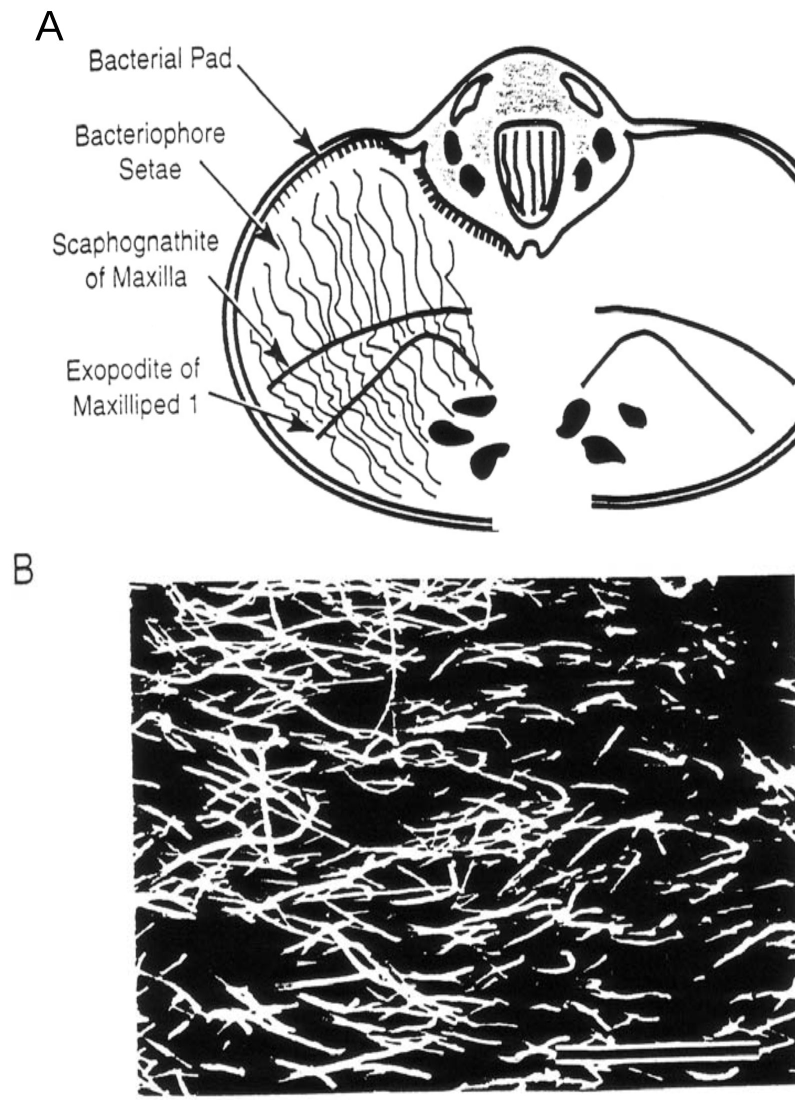

Figure 8.8. A. Schematic cross-section of *Rimicaris exoculata* at the level of the branchial chambers, illustrating the location of episymbiotic bacteria as a bacterial pad and on bacteriophore setae of the maxillal scaphognathite and exopodite of maxilliped I. From Segonzac et al. 1993. B. Scanning electron micrograph of the pad of filamentous bacteria found on the dorsal inner surface of the branchial chamber of *Rimicaris exoculata*. Scale bar = 100 µm. Photo by C. L. Van Dover.

TABLE 6.2.
Invertebrate–chemo(or methano)autotrophic symbioses

Host Taxonomy	*Endo- or Episymbiont*	*Symbiont Location*	*Symbiont Autotrophic Condition*	*Adult Digestive System*
Porifera				
Family Cladorhizidae	endosymbiont	"sponge tissue"	methanotrophic	nonexistent
Nematoda				
Subfamily Stilbonematinae	episymbiont	cuticle, intraepidermal	thiotrophic	functional
	endosymbiont	intestinal intracellular	thiotrophic	functional
Mollusca				
Class Bivalvia:				
Family Vesicomyidae	endosymbiont	gills	thiotrophic	nonfunctional
Family Mytilidae	endosymbiont	gills	thio- and methanotrophic	functional
Family Pectinidae	endosymbiont	gills	presumed thiotrophic	functional
Class Gastropoda:				
Family Provannidae	endosymbiont	gills	thio- and ?methanotrophic	functional
Echiura	endosymbiont	intraepidermal	thiotrophic	functional
Annelida				
Class Polychaeta				
Family Alvinellidae	episymbiont	dorsal surface	thiotrophic	functional
Class Oligochaeta				
Subfamily Phallodrilinae	endosymbiont	subcuticular	thiotrophic	functional
Vestimentifera	endosymbiont	trophosome	thiotrophic	lost
Pogonophora	endosymbiont	trophosome	thio- and methanotrophic	lost
Arthropoda				
Family Alvinocaridae	episymbiont	branchial chamber	thiotrophic	functional

From references cited in text.

Van Dover, 2000

Vents are dynamic – blink on and off on decadal time scales

Tunnicliffe, 1991

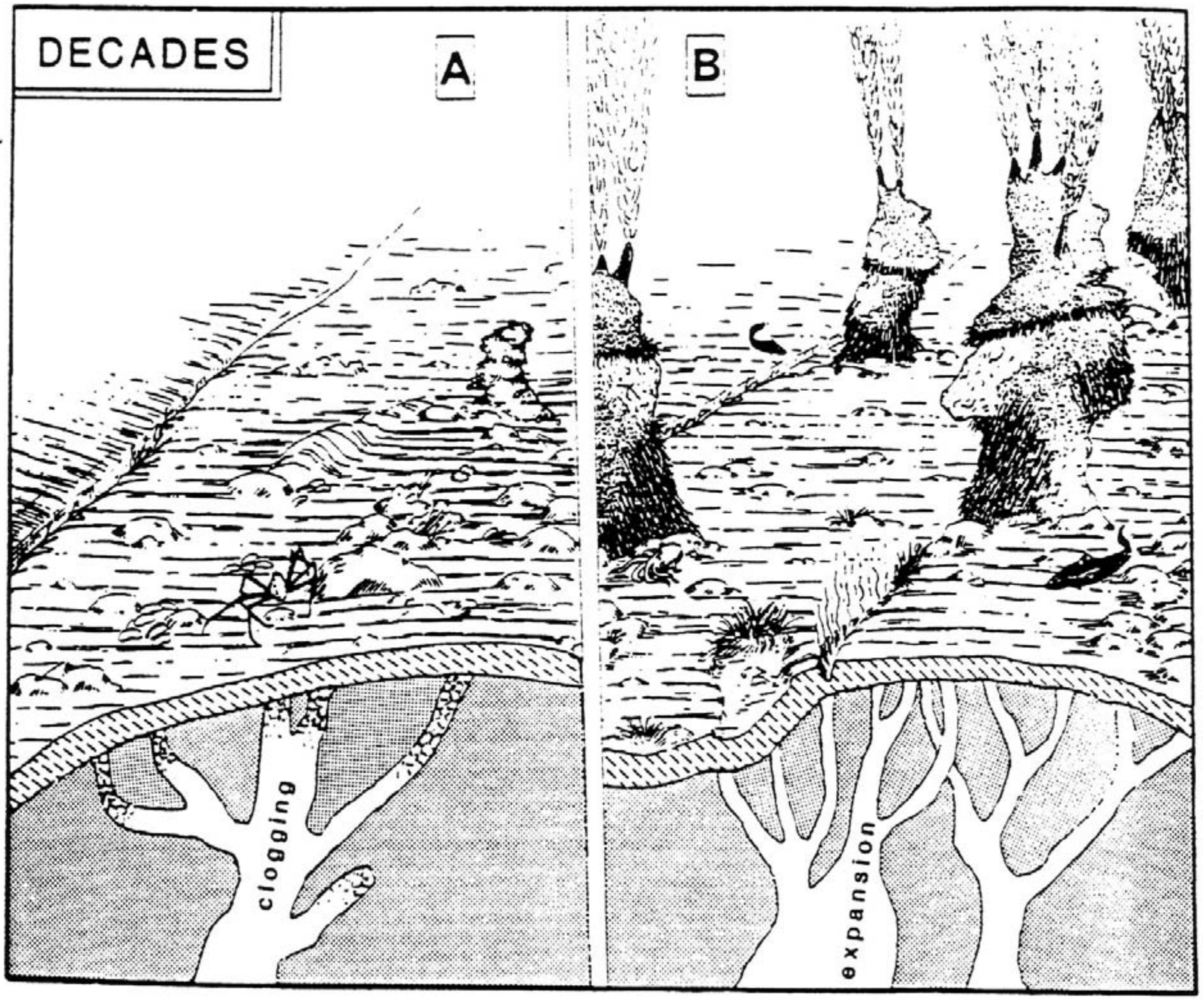

Fig 11.—Representation of the long-term changes that may occur within a vent field. Over decades, the subsurface fluid conduits may become clogged by either sulphide deposits or tectonic shifts thus resulting in the extinction of a field (A). Expansion of the plumbing system is also possible resulting in large scale smoker growth and or field extension (B).

TABLE III

Estimates of growth rate and age in the giant clam *Calyptogena magnifica* as made by a variety of methods. All specimens are from either Galapagos Rift or from 21°N EPR. * = dead on collection. ** = maximum ages interpreted from published growth curves by present author

Number of specimens max. size	Rate	Max. age yr	Technique	Reference
1 22 cm	4 cm/yr	6.5	$^{228}Th/^{228}Ra$	Turekian, Cochran & Nozaki, 1979
1 19 cm	5–6 cm/yr	3–4	$^{228}Th/^{228}Ra$ $^{210}Po/^{210}Pb$	Turekian & Cochran, 1981
1 21.5 cm	0.58 cm/yr	37	$^{228}Th/^{228}Ra$	Turekian, Cochran & Bennett, 1983; Lutz, Fritz & Rhoads, 1985
1 12.5 cm	1.2 cm/yr over 3 yr	10 +	Stable isotope comparisons	Roux *et al.*, 1983
58 25.1 cm	0.8–1.1 cm/yr	23–37	Shell dissolution calculation	Rio & Roux, 1984
28 21 cm	log. decrease with size	16–25**	Shell dissolution calculations	Lutz, Fritz & Rhoads, 1985
90 22 cm*	log. decrease with size	≈19 (Galap) ≈40 (21°N)	Shell dissolution calculations	Lutz, Fritz & Cerrato, 1988
30 21.9 cm	log. decrease with size	19.6	Modified Lutz *et al.* growth model	Fisher *et al.*, 1988a

Tunnicliffe, 1991

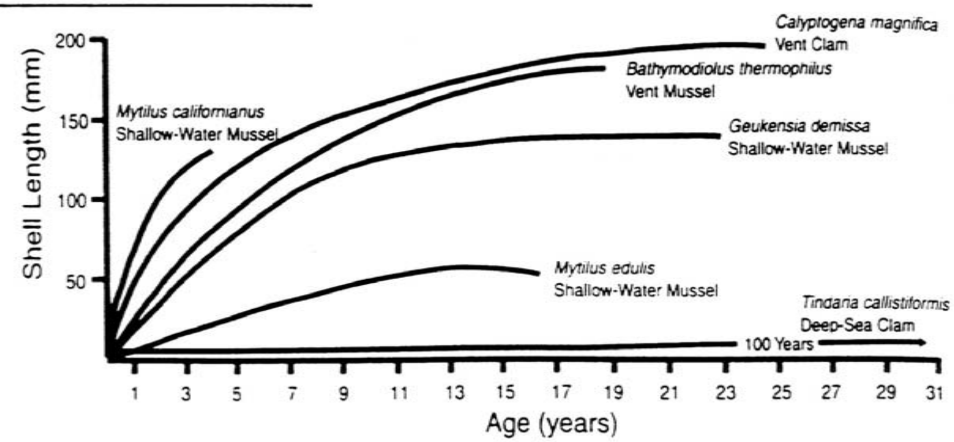

Figure 7.14. Growth curves for various species of bivalves. Note that the vent clam (*Calyptogena magnifica*) and mussel (*Bathymodiolus thermophilus*) have growth curves comparable to those of shallow-water mussel species (*Mytilus californianus*, *Geukensia demissa*), while the non-vent deep-sea clam *Tindaria callistiformis* has an extremely slow growth rate. From Turner and Lutz 1984.

Van Dover, 2000

TABLE II

Enzyme Activities of the Calvin-Benson Cycle, Sulfur Metabolism, and Nitrate Reduction in Marine Animals from Habitats in Which Sulfide and Oxygen Are Both Available

Species (phylum) and habitat	Enzyme activities[a]					
	Calvin–Benson cycle		Sulfur metabolism			Nitrogen metabolism
	RuBPCase	Ru-5-P Kinase	ATP-Sulfurylase	APS-Reductase	Rhodanese	Nitrate reductase
Rift vents						
Riftia pachyptila (Pogonophora)	0.22	19.01	74.0	7.6	7.6	0.07
Riftia sp. (Guaymas basin species)	1.13	—	133.0	30.1	5.2	0.34
Calyptogena magnifica (Mollusca)	0.4	—	—	—	—	—
Vent mytillid (unnamed, Mollusca)	0.05	—	—	—	—	—
Fault vent (San Diego Trough)						
Lamellibrachia barhami + unnamed species (Pogonophora)	0.4	—	30.0	—	—	—
Calyptogena pacifica (Mollusca)	0.6	—	25.0	—	—	—
Sewage outfall						
Solemya reidi + *S. panamensis* (Mollusca)	2.4	4.4	77.0	4.1	0.7	0.23
Parvilucina tenuisculpta (Mollusca)	0.01	—	3.8	—	—	0.08
Santa Barbara Basin						
Lucinoma annulata (Mollusca)	0.1	1.25	0.6	—	—	—
Eelgrass beds						
Solemya velum (Mollusca)[b]	+	—	—	—	—	—
Mangrove swamps						
Codakia obicularis[c]	0.2	—	43.0	—	—	1.4
Lucina pennsylvanica[c]	+	—	—	—	—	—

[a] Data from Felbeck et al. (1981) unless otherwise indicated. Enzyme activities are expressed as micromoles of substrate converted to product per minute per gram fresh weight of tissue, at a measurement temperature of 20–25°C. The plus (+) symbol indicates instances where the enzyme was detected, but quantitation of activity was not obtained or reported.

[b] Data from Cavanaugh (1980).

[c] Unpublished data of H. Felbeck and C. Berg.

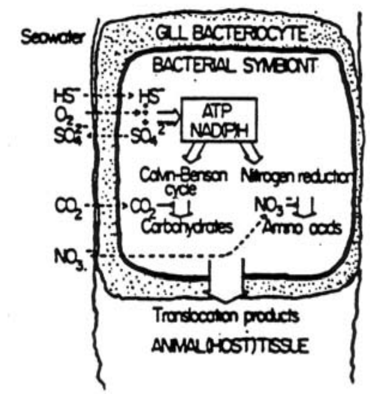

Fig. 1. A diagrammatic presentation of the metabolic organization found in the gills of bivalves harboring sulfide-oxidizing symbiotic bacteria. This metabolic organization has three major components: (1) sulfide oxidation with concomitant synthesis of ATP and reducing power (NAD(P)H); (2) reduction of CO_2 and nitrate (Calvin–Benson cycles and nitrate-reducing reactions, respectively); and (3) translocation processes that supply the host with reduced carbon and nitrogen compounds that are synthesized within the symbiotic bacteria.

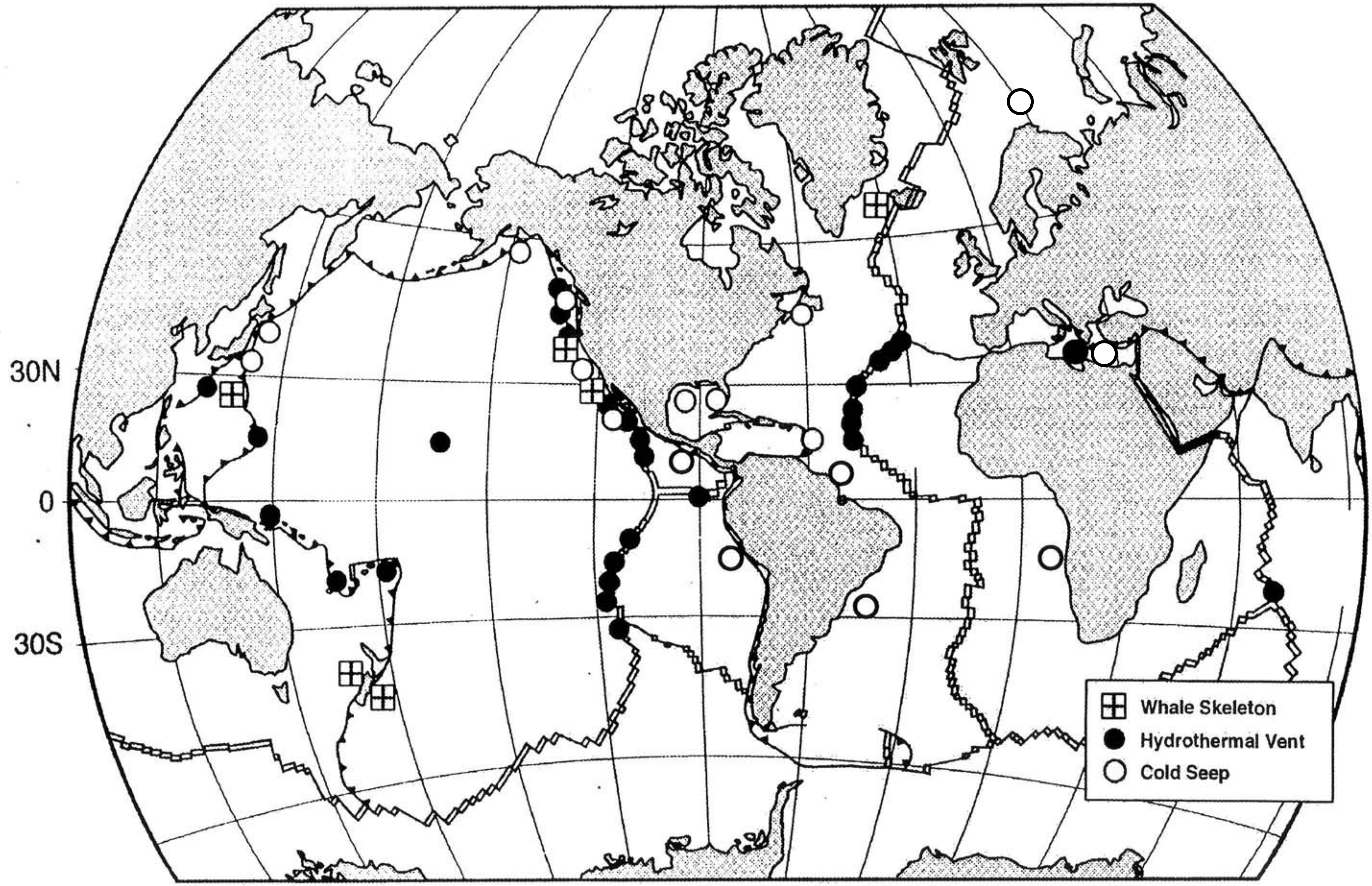

Known vent seep and whale-fall sites (after Smith and Baco, 2003)

Subduction Zones

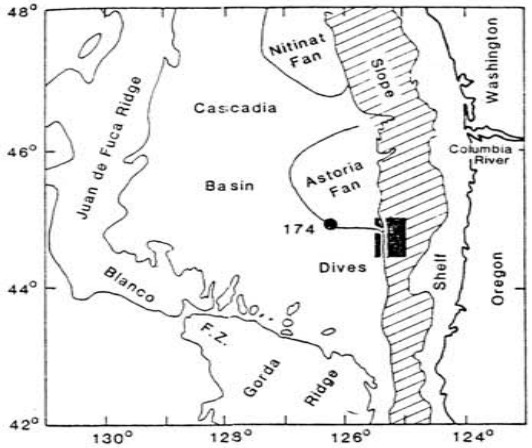

Fig. 1. Oregon subduction zone (lined pattern), Juan de Fuca pla (Cascadia Basin), and Astoria Fan. The dive area is shown by the black bo Deep Sea Drilling Project drill site 174.

Fig. 3. Composite illustration of vent site 1428 (*11*). Two colonies of tube worms, *Lamellibrachia barhami*, occur on the ledge above the canyon wall; several clusters of live giant clams, *Calyptogena* sp., are aligned along presumed sites of fluid discharge; an open valve of *Solemya* sp. is seen on the far right; and a cone-shaped chimney structure is shown at the top. Carnivorous fishes and large crabs are attracted to the clam beds. Venting sites are at least 20 m² in areal extent. [Courtesy of the Biological Society of Washington]

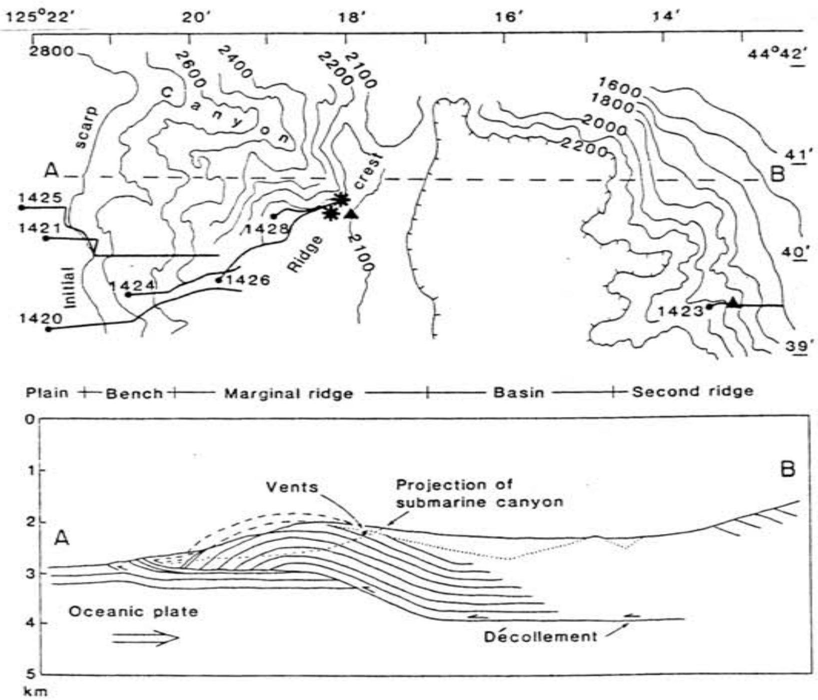

Fig. 2. (Top) *Alvin* dive transects and SeaBeam bathymetry map obtained by the National Oceanic and Atmospheric Administration, National Ocean Survey, aboard the *Surveyor* of the Oregon underthrust region. Contours are in meters: numbered dives commence at the solid dots. Asterisks indicate fluid vent sites (northern site 14[illegible] and southern site 1426); triangles indicate car[illegible] chimneys at both vent sites and along dive transect 1423. (Bottom) Interpretive structural section of the deformation front along profile A–B (dashed line). This depth section was compiled from seismic refraction and reflection data and bedding dips measured from *Alvin*; oceanic crust here is at 7-km depth.

Other examples:

Japan and Peru trenches, Barbados prism

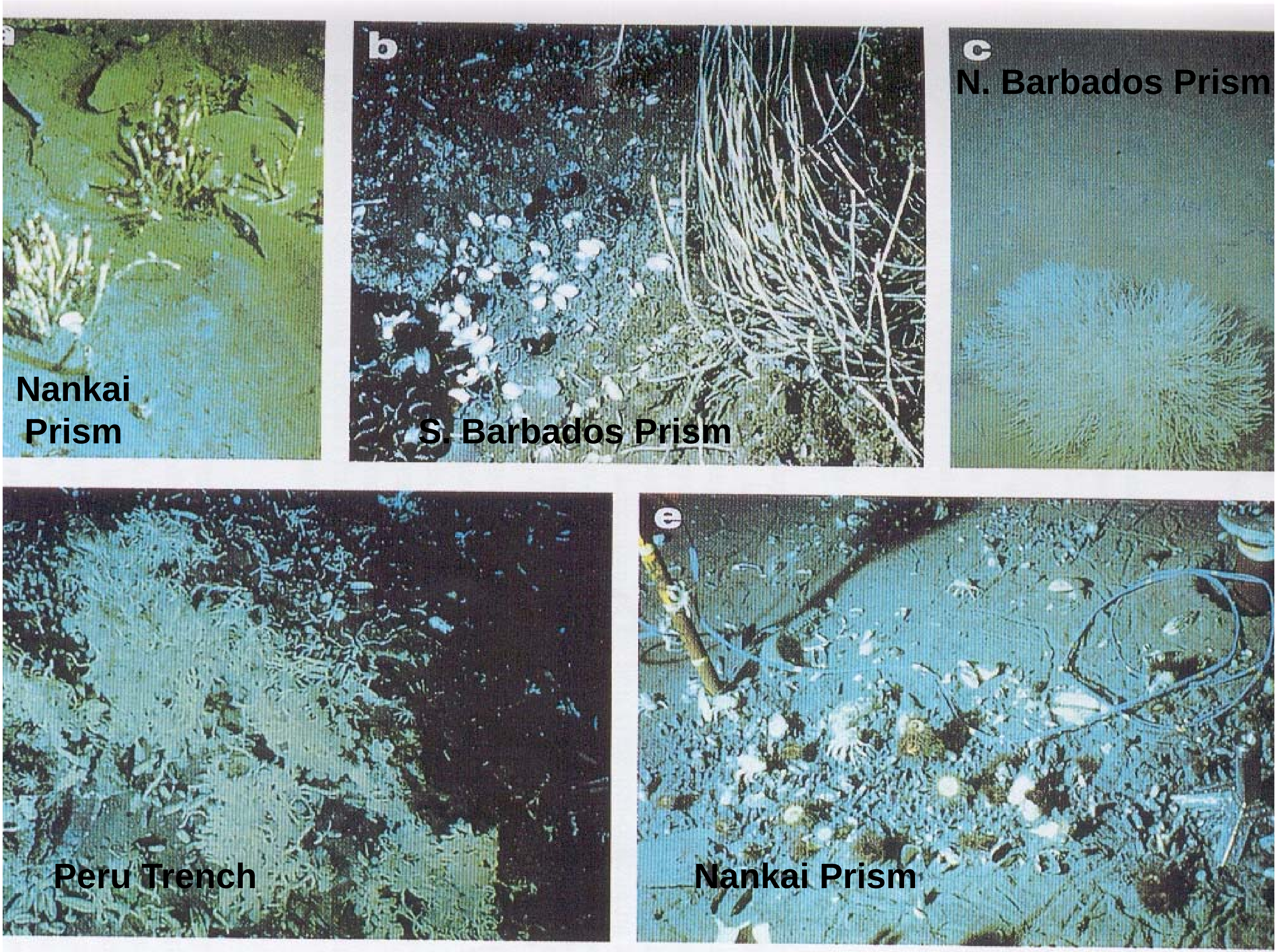
a
Nankai
Prism
b
S. Barbados Prism
c
N. Barbados Prism
Peru Trench
e
Nankai Prism

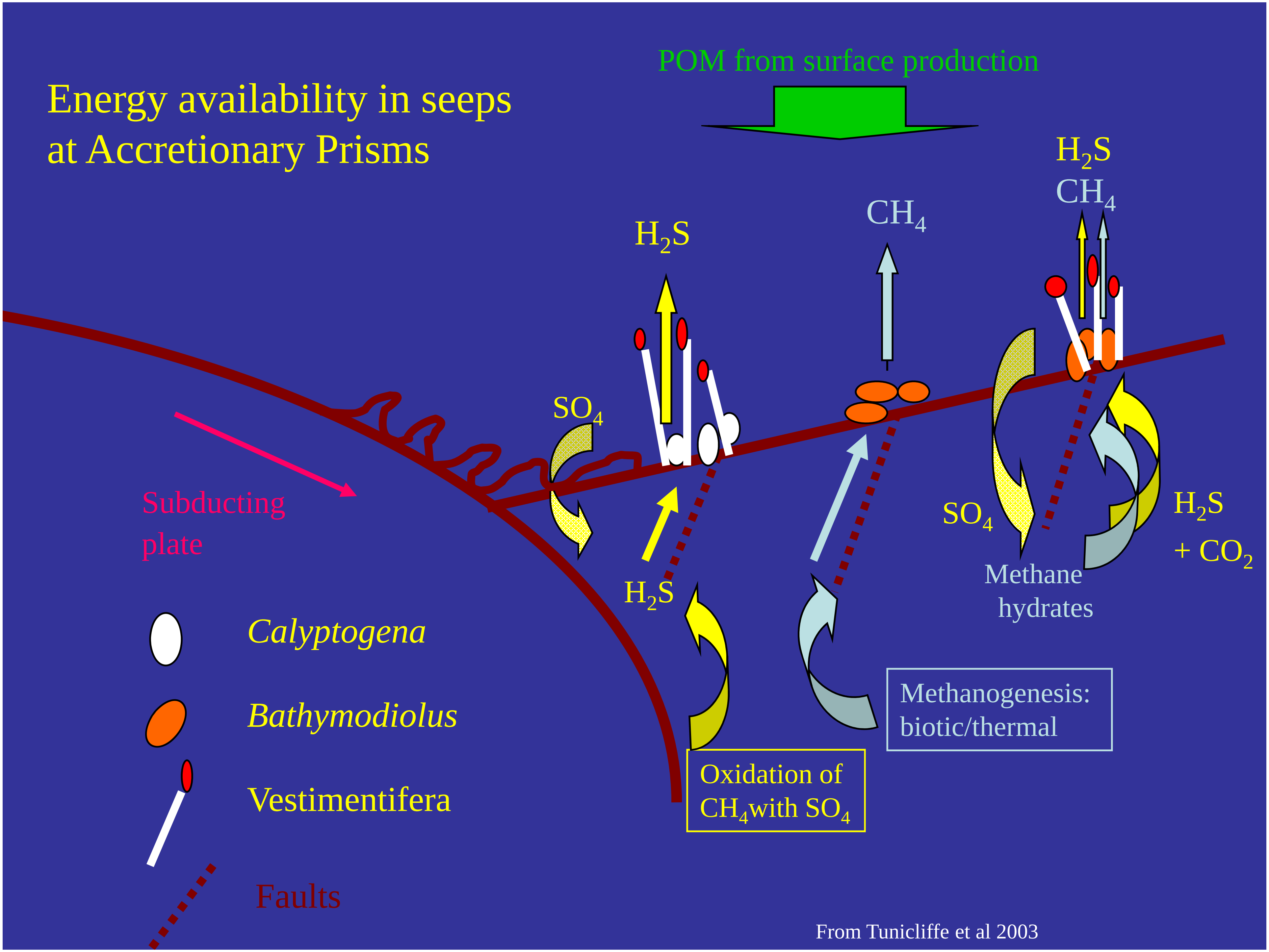

Energy availability in seeps at Accretionary Prisms
POM from surface production
H_2S
CH_4
H_2S
CH_4
SO_4
H_2S
SO_4
H_2S + CO_2
Methane hydrates
Subducting plate
Calyptogena
Bathymodiolus
Vestimentifera
Faults
Methanogenesis: biotic/thermal
Oxidation of CH_4 with SO_4
From Tunicliffe et al 2003

Petroleum and Hydrocarbon seeps (including methane hydrates)

E.g., Gulf of Mexico, Angola and Brazil margins,

1642 M. C. KENNICUTT II *et al.*

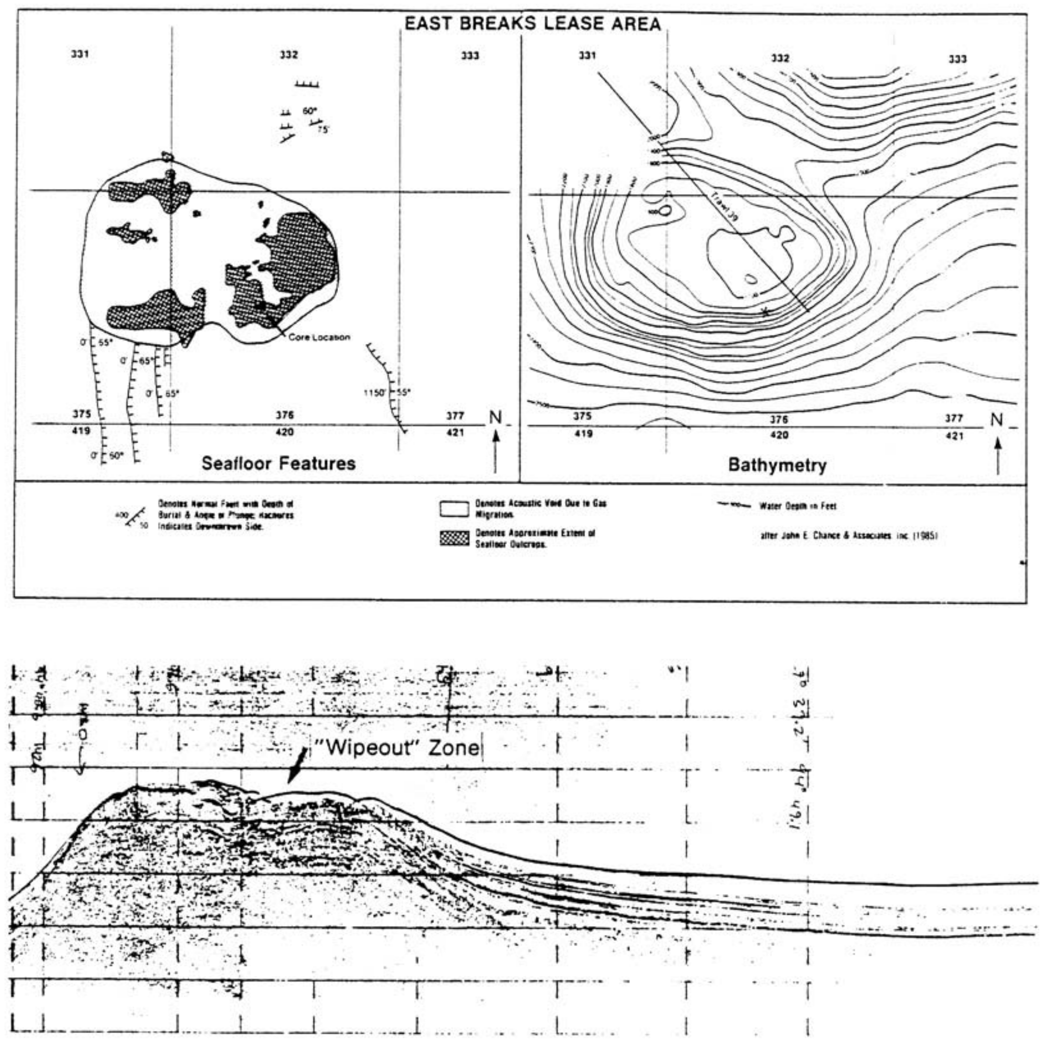

Fig. 1. Shallow seafloor features, bathymetry and 3.5 kHz sub-bottom profile for the trawl line at EB-376.

<u>Petroleum and Hydrocarbon seeps (including methane hydrates)</u>

E.g., Gulf of Mexico,
Angola and Brazil margins,

Louisiana Slope, Gulf of Mexico

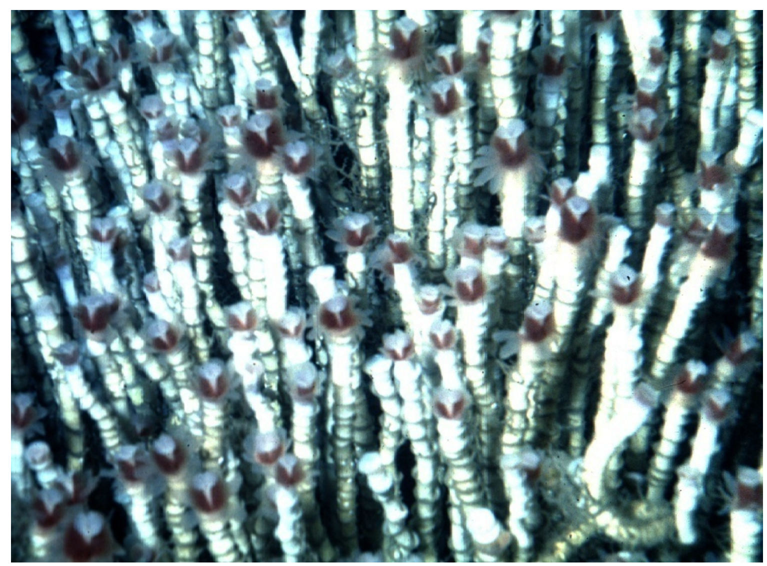

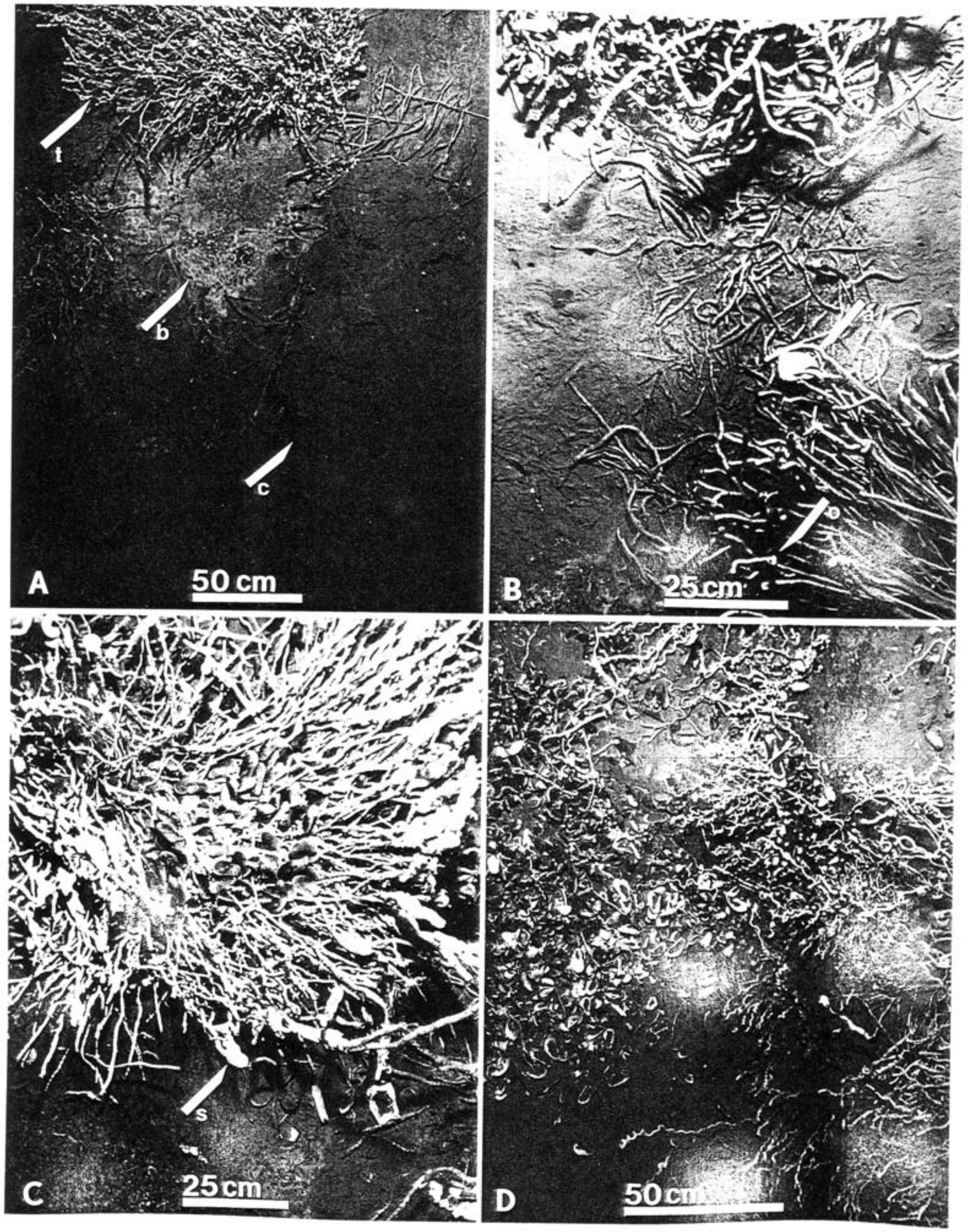

Fig. 3. Photographs taken with vertically-mounted 35 mm camera. (A) Bush-like clusters of *Lamellibrachia* sp. (t), carbonate boulder (c) and bacterial mat (b). (B) Small tangle of *Lamellibrachia* sp. with attached *Acesta bullisi* (a), obturacular plume of *Lamellibrachia* sp. (o) and an escarpiid vestimentiferan (e). C: Basket-like cluster of *Lamellibrachia* sp. with seep mussels in center, epifaunal sponge (s). D: Transition between bed of seep mussels and sparse clusters of *Lamellibrachia* sp.; note dead mussels shells

Louisiana Slope, Gulf of Mexico

Utilization of methane at cold seeps

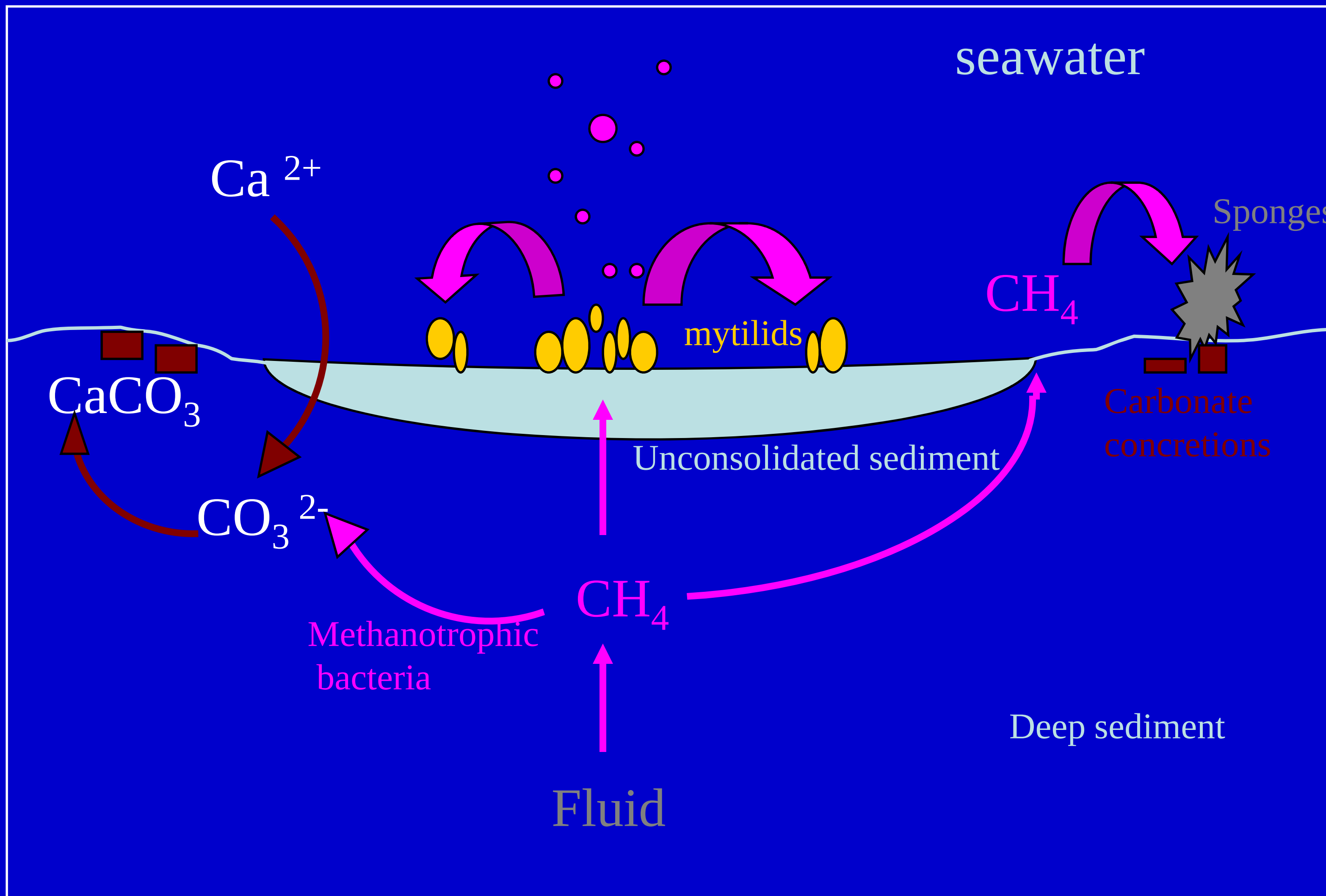

Formation and utilization of sulphides

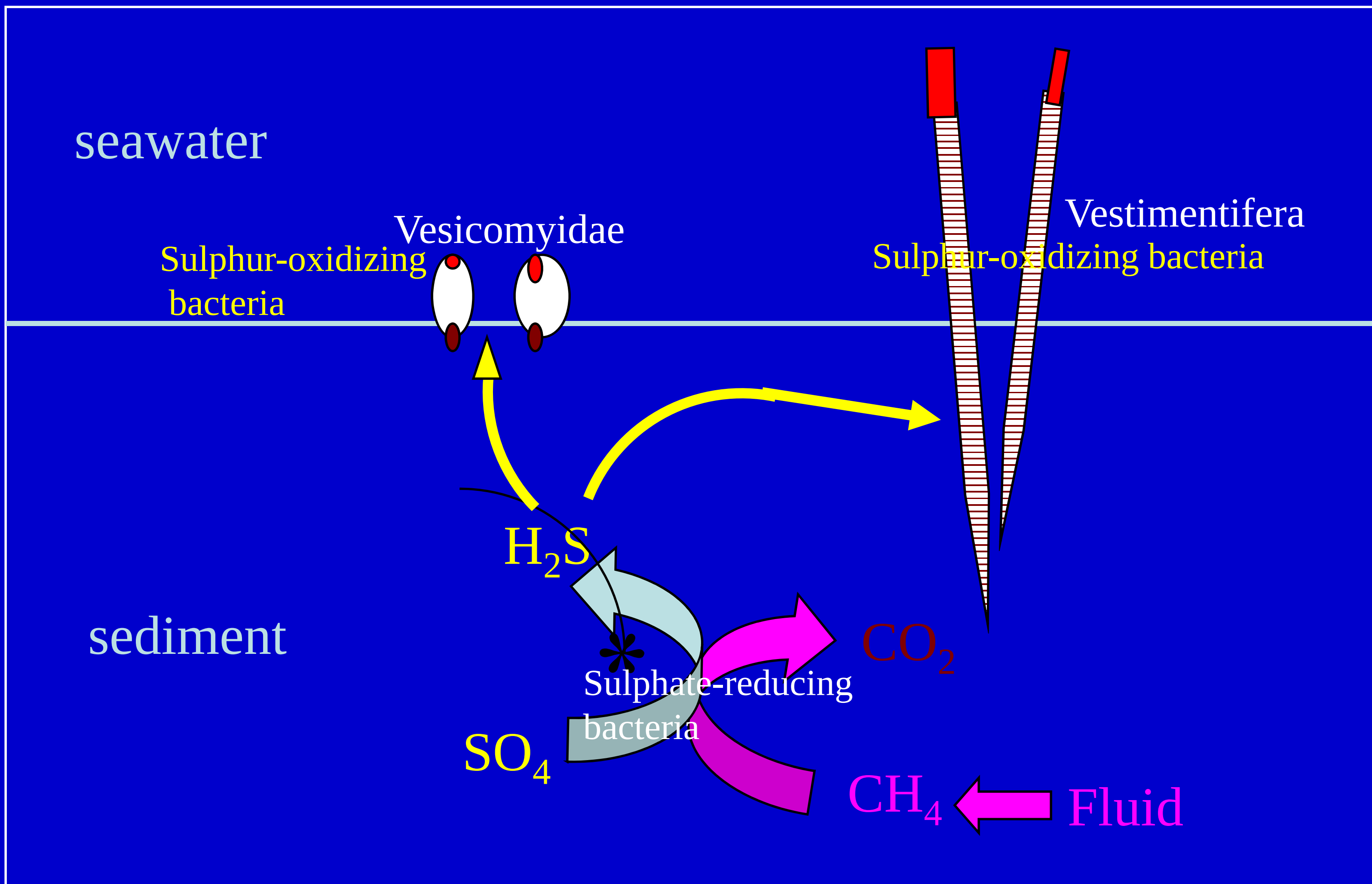

Hesiocaeca methanicola: the ice worm

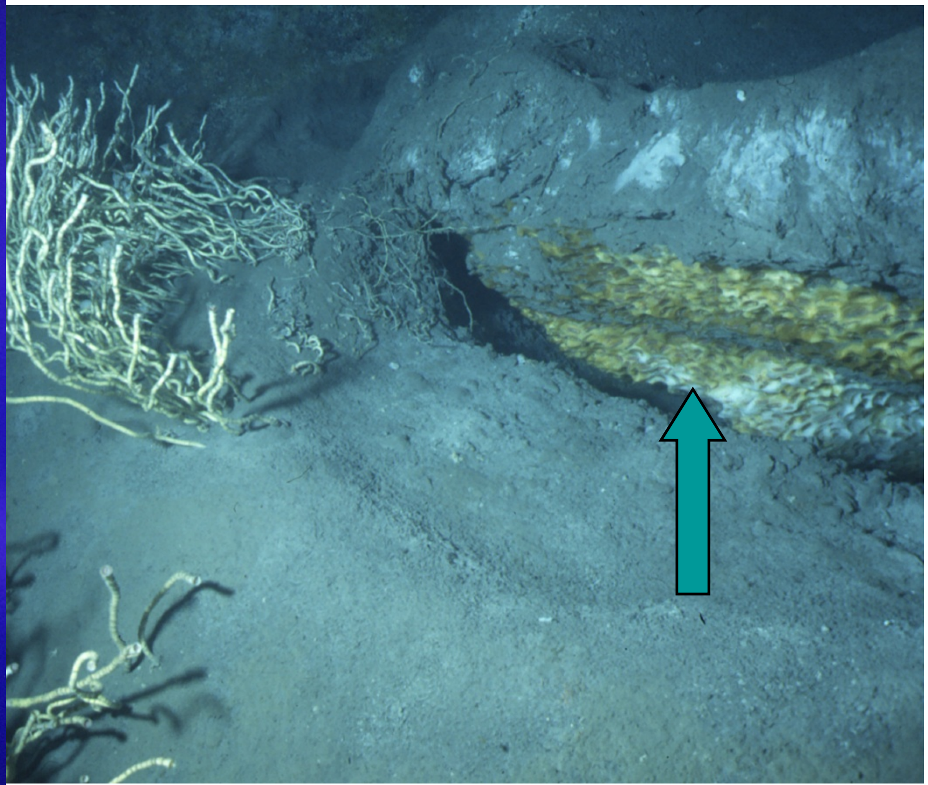

Phase diagram for
methane in pure water
The methane hydrate
forms below
the sediment-water
interface where
temperature/pressure
conditions are right
for hydrate formation

From Kvenvolden 1988

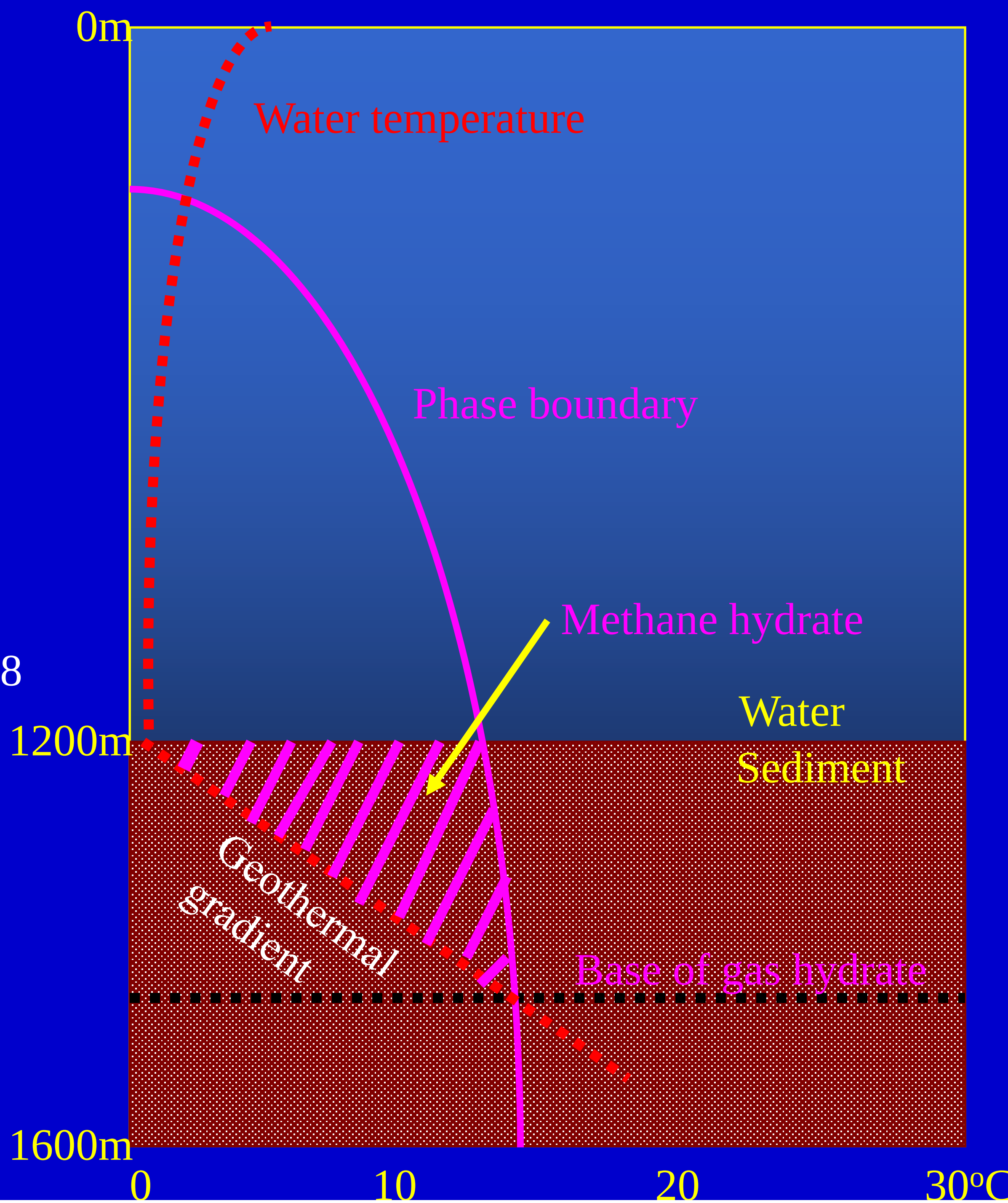

Brine seepage:

Louisiana slope,
Florida escarpment,
Monterey canyon

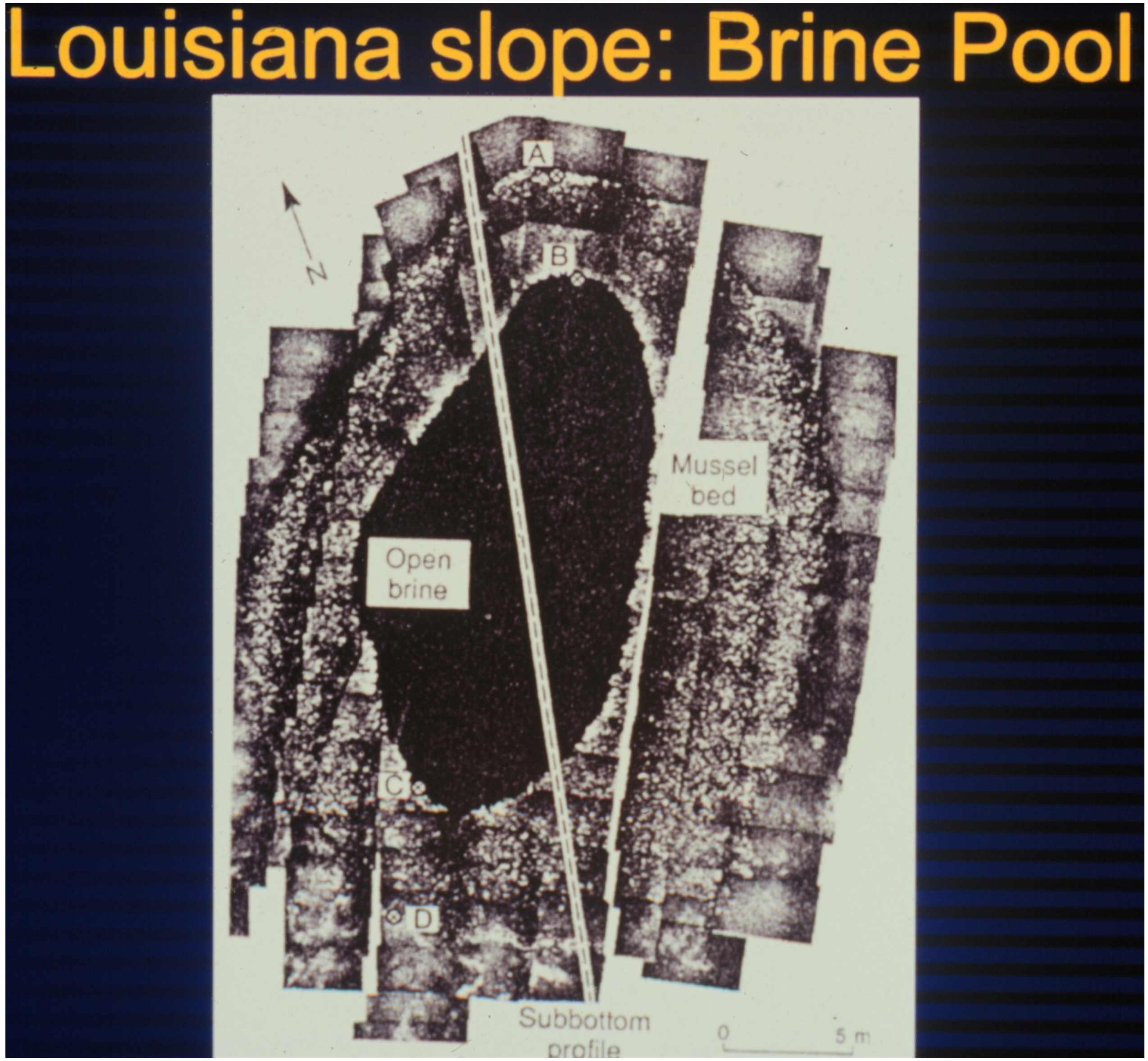

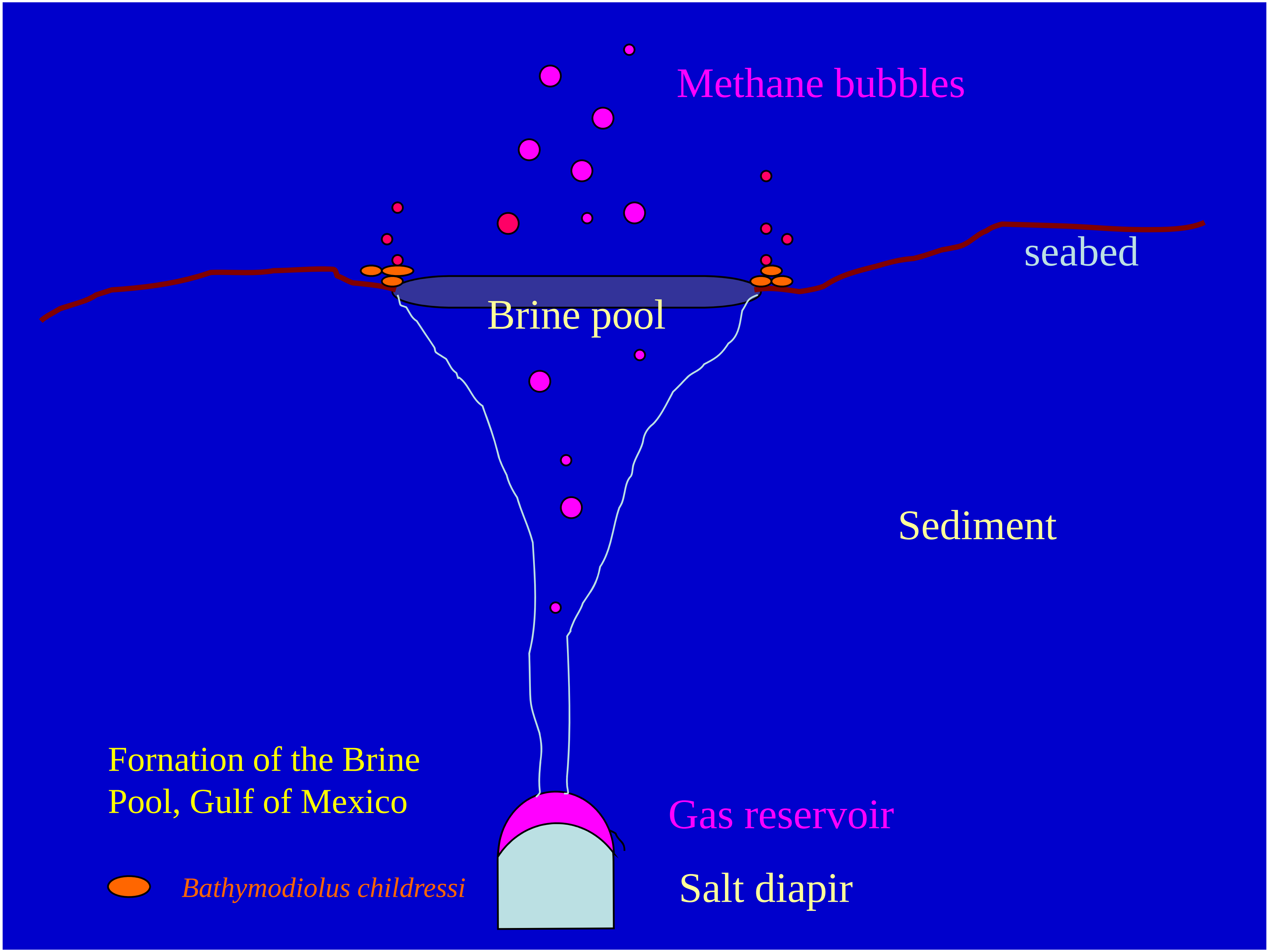
Methane bubbles
seabed
Brine pool
Sediment
Fornation of the Brine
Pool, Gulf of Mexico
Gas reservoir
Bathymodiolus childressi
Salt diapir

Turbidites and Slump Scarps

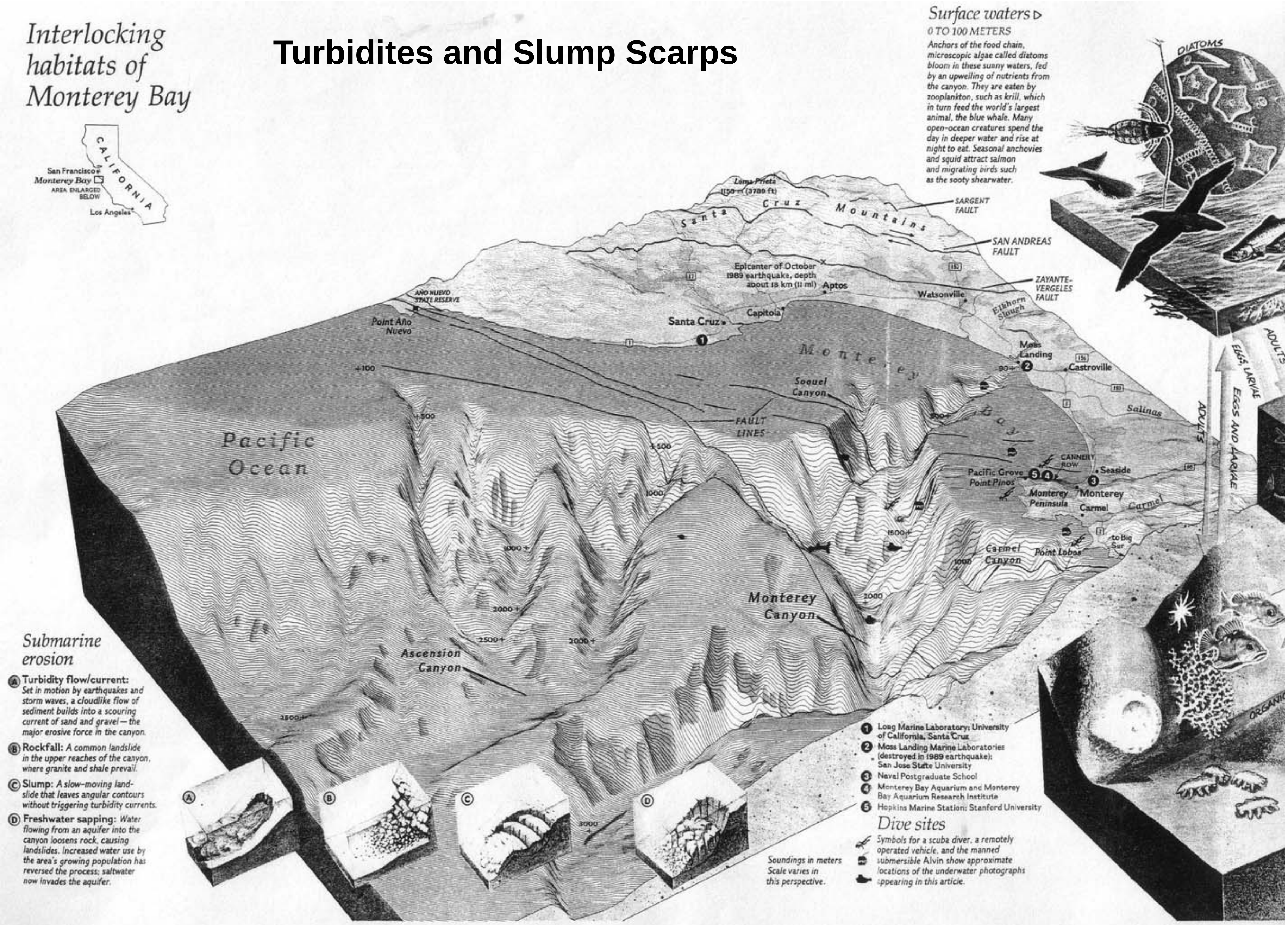

Mud Volcanoes

Barbados,
Norway (Hakon Mosby),
Mediterranean

Barbados Accretionary Prism: Distribution of clams

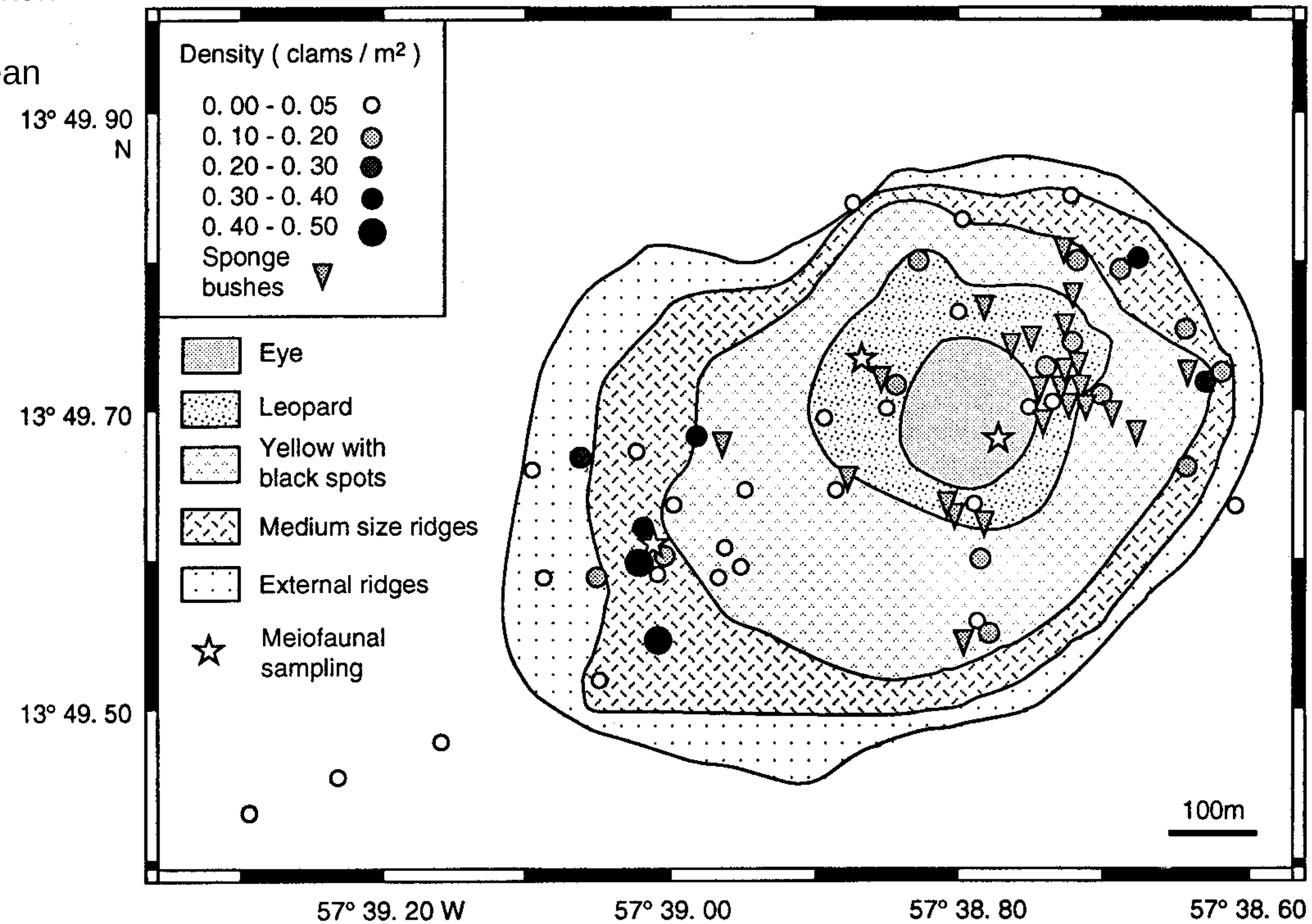

Model of fluid flow and animal distribution round a mud volcano on the Barbados accretionary prism

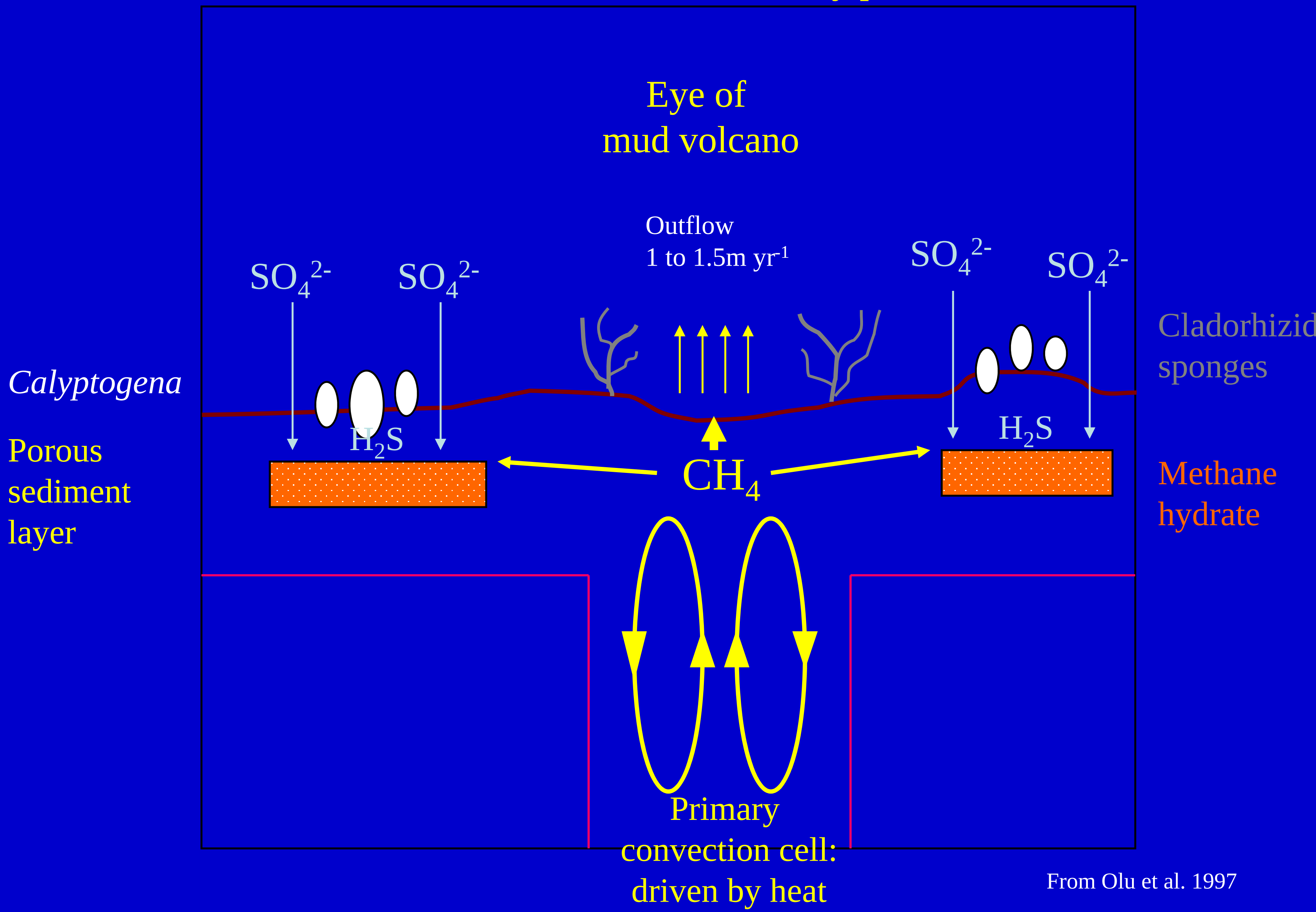

From Olu et al. 1997

Whale falls

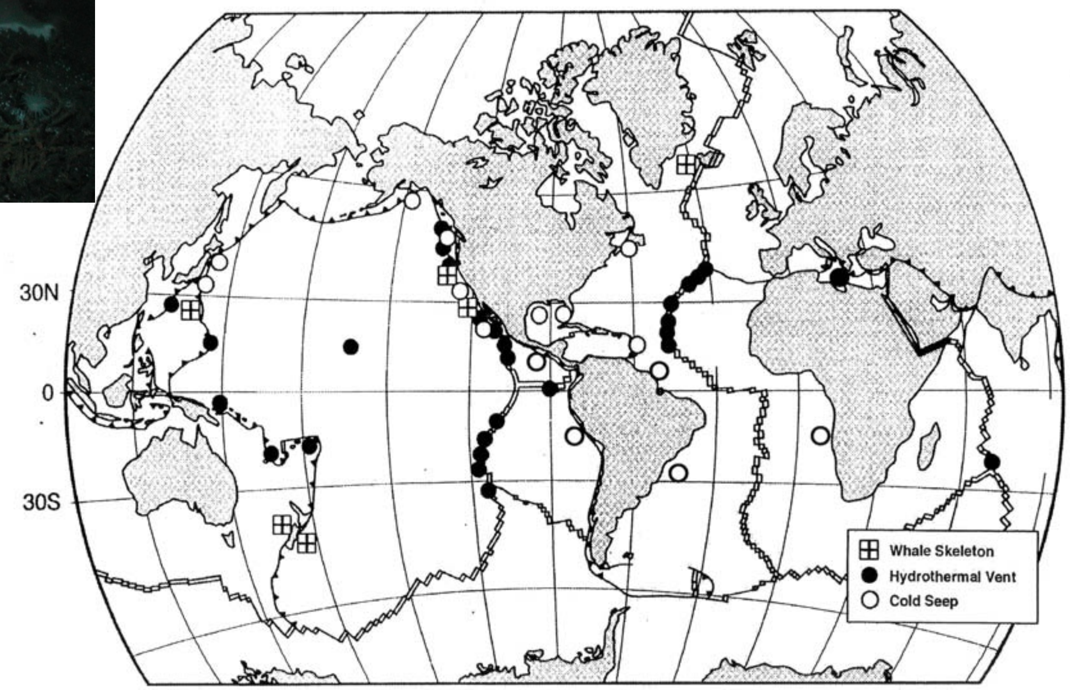

Known vent seep and whale-fall sites (after Smith and Baco, 2003)

Bone-eating "zombie worms" ≥ 8 species

Monterey Canyon - *O. rubiplumus* & *O. frankpressi*

(Rouse et al. 2004)

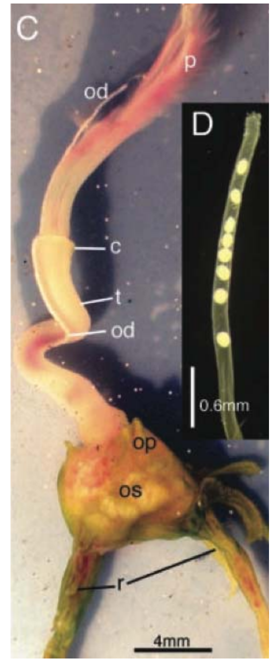

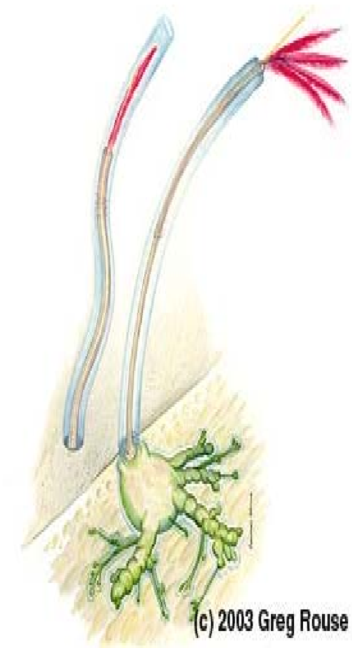

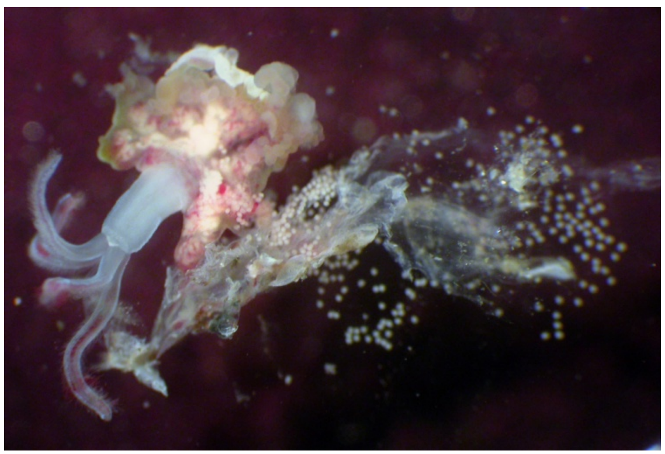

Santa Cruz Basin - *Osedax* sp. n.

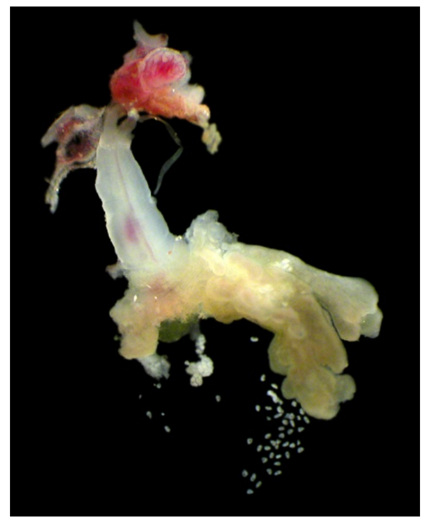

Sweden

→ **World Wide Whale Worms?**

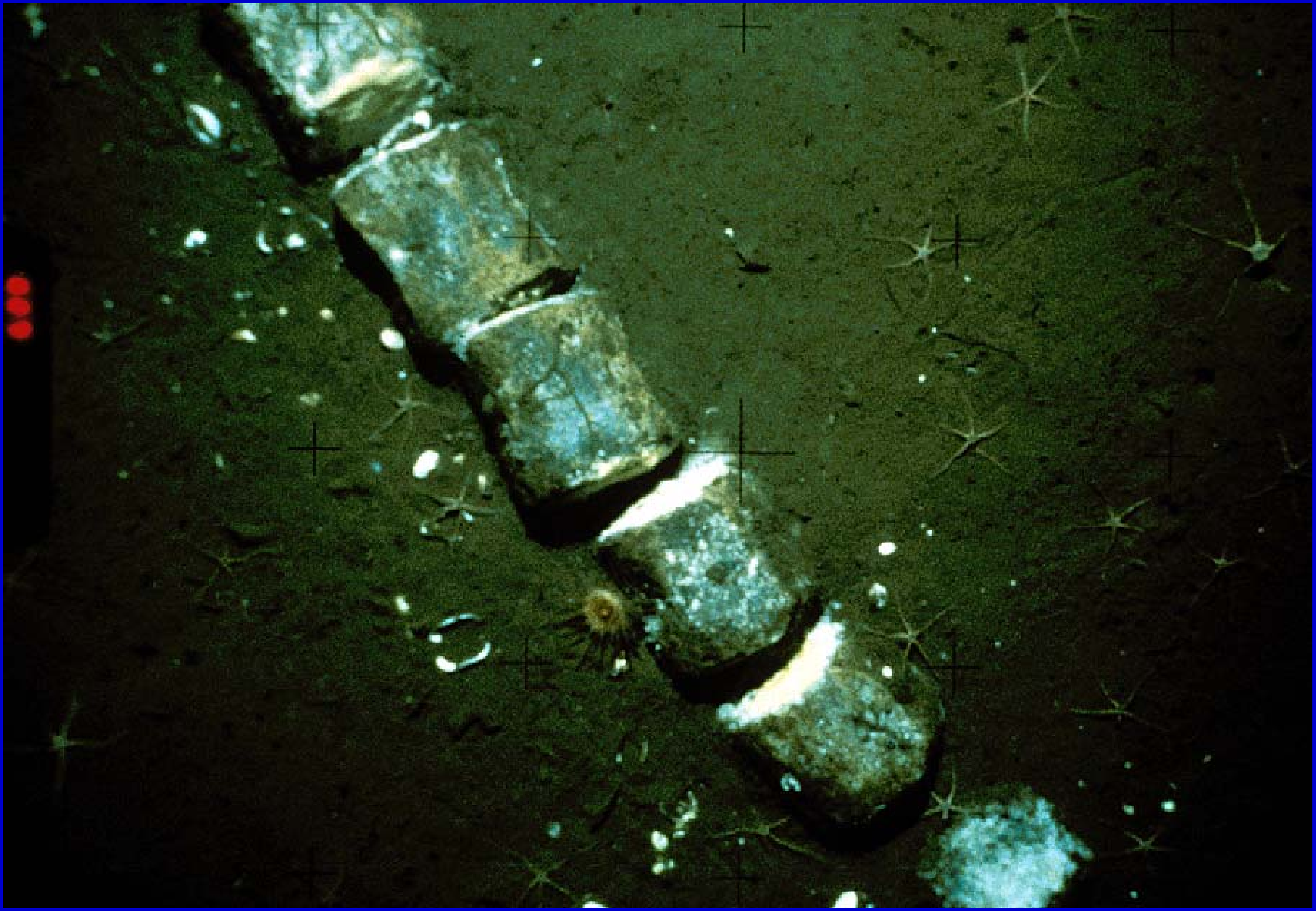

Blue whale vertebrae, vesicomyid clams & bacterial mats – Santa Catalina Basin

Idas washingtonia and *Cocculina craigsmithi*

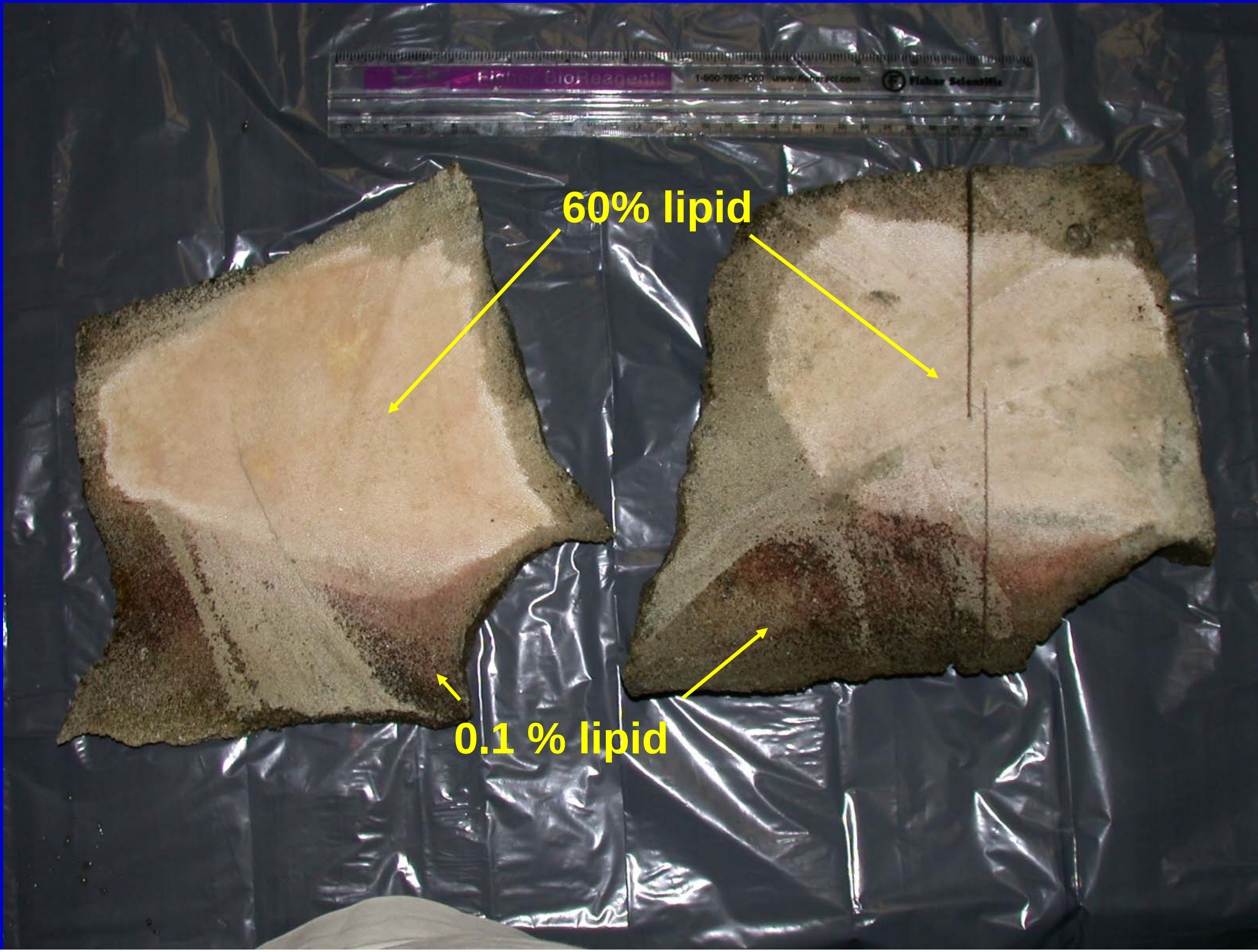

60% lipid
0.1 % lipid

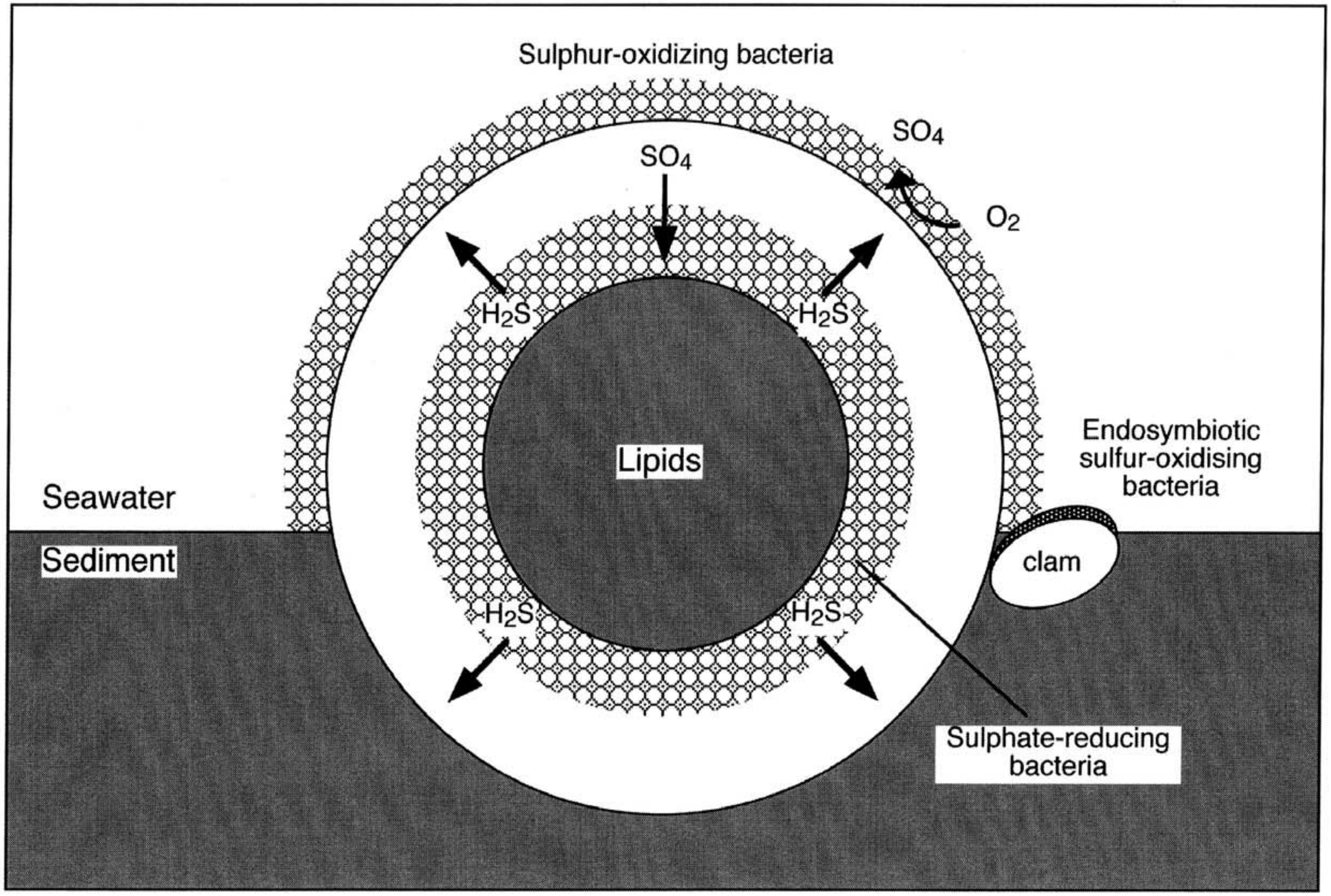

igure 6. Schematic cross section of a whale vertebra resting at the seafloor during the *sulphophilic stage* of succession. The redominant decompositional processes occurring within in the bones are illustrated, which include: (1) Diffusion of sulphate from eawater into the bone; (2) Sulphate reduction by anaerobic bacteria decomposing lipids in the lipid-rich bone core; (3) Diffusion of

Smith and Baco, 2003

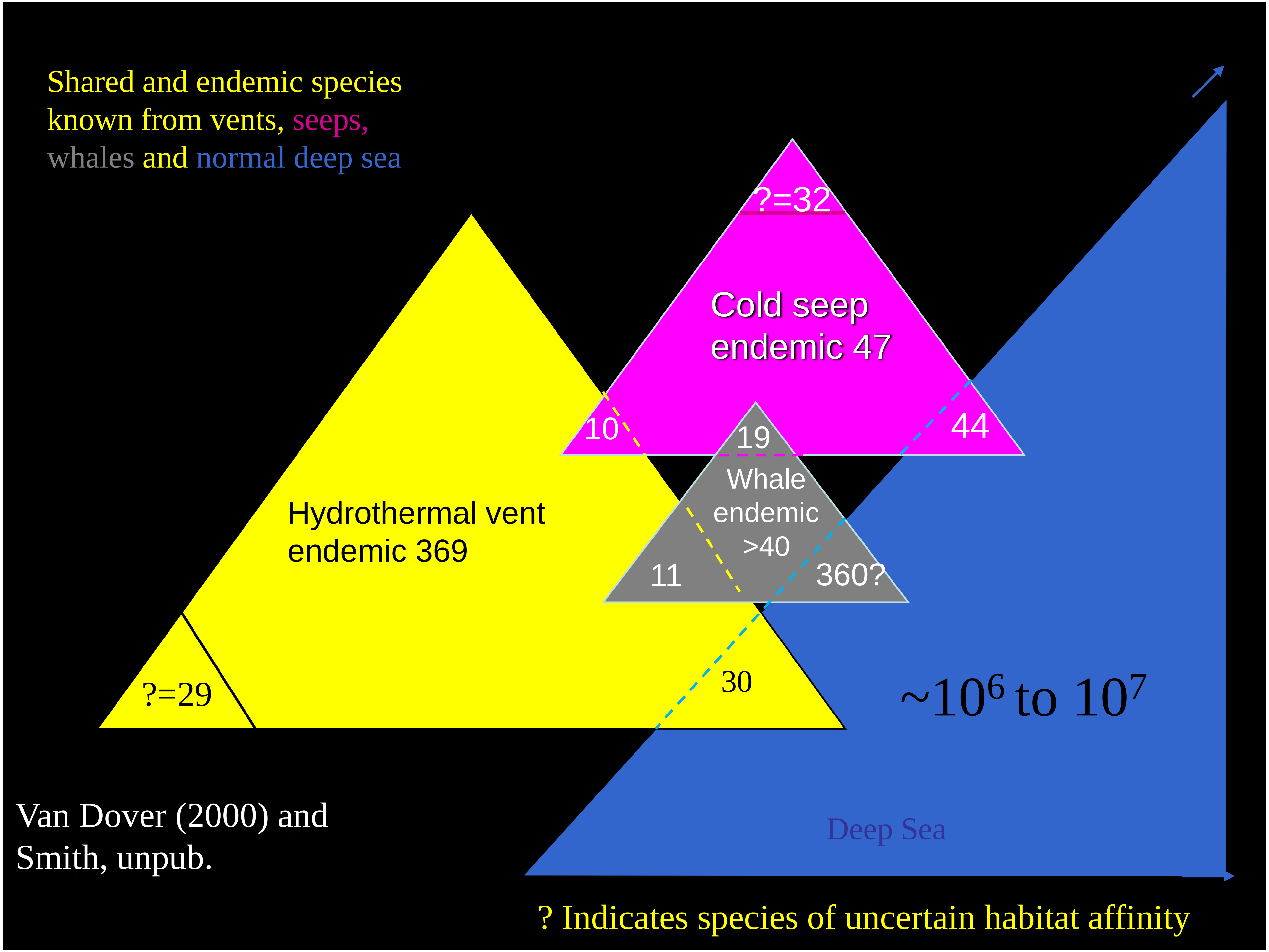
Shared and endemic species known from vents, seeps, whales and normal deep sea
?=32
Cold seep endemic 47
10
19
44
Whale endemic >40
11
360?
Hydrothermal vent endemic 369
?=29
30
~10^6 to 10^7
Deep Sea
Van Dover (2000) and Smith, unpub.
? Indicates species of uncertain habitat affinity

Van Dover, 2000

TABLE 12.1.
Sulfide and methane concentrations measured at various seep and other reducing environments

Setting	Hydrogen Sulfide Concentration	Methane Concentration	Reference
Atlantic			
Florida Escarpment	5.7 mM	10 mM	Chanton et al. 1991
Bush Hill (Louisiana Slope)	11 µM	60 µM	MacDonald et al. 1989, 1990a
Laurentian Fan	43–49 µM (top 1 cm)	not available	Mayer et al. 1988
	183 µM (> 1 cm)	not available	Mayer et al. 1988
Barbados Accretionary Prism	not available	500 µM	Blanc et al. 1988
North Sea Pockmark	not detectable	<4 nM dm^{-} (upper 10 cm)	Dando et al. 1991
		237 nM dm^{-3} (30 cm)	Dando et al. 1991
Skagerrak Methane Seep	500 µg-at. S l^{-1}	3.4 mM dm^{-3} (upper 10 cm)	Dando et al. 1994
Western Pacific			
Nankai Trough	2–4000 nM	5–7 × 10^{-5} M (clams present)	Gamo et al. 1992; Fiala-Médioni et al. 1993
		0.1–1.3 × 10^{-2} M (clams absent)	
Sagami Bay		10,000 nl kg^{-1}	Sakai et al. 1987
Eastern Pacific			
Monterey Canyon	0.6–19.4 mM	0–841 µM	Barry et al. 1997a
Northern California Methane-Hydrate Field	not available	10,000 µl l^{-1}	Kennicutt et al. 1989
Gulf of Alaska			
Aleutian Subduction Zone	4.6 mM (25–30 cm)	0.35 mM (35 cm)	Wallman et al. 1997
Whale Skeletons			
Santa Catalina	10-20 mM	not available	Smith et al. 1989
Torishima Seamount	20 nM	not available	Naganuma et al. 1996